

Electronic Acknowledgement Receipt

EFS ID:	7165042
Application Number:	61311672
International Application Number:	
Confirmation Number:	7500
Title of Invention:	DOUBLE-DUCTED FAN
First Named Inventor/Applicant Name:	Cengiz Camci
Customer Number:	86002
Filer:	Amy Amber Dobbelaere/Sarah Scott
Filer Authorized By:	Amy Amber Dobbelaere
Attorney Docket Number:	6460-94
Receipt Date:	08-MAR-2010
Filing Date:	
Time Stamp:	18:02:28
Application Type:	Provisional

Payment information:

Submitted with Payment	yes
Payment Type	Credit Card
Payment was successfully received in RAM	\$110
RAM confirmation Number	5133
Deposit Account	141437
Authorized User	DOBBELAERE,AMY

The Director of the USPTO is hereby authorized to charge indicated fees and credit any overpayment as follows:

Charge any Additional Fees required under 37 C.F.R. Section 1.17 (Patent application and reexamination processing fees)

Charge any Additional Fees required under 37 C.F.R. Section 1.21 (Miscellaneous fees and charges)

File Listing:

Document Number	Document Description	File Name	File Size(Bytes)/Message Digest	Multi Part /.zip	Pages (if appl.)				
1		6460-94_PROVAPPLICATION.pdf	10838839 0aaa7e644cc1871eb30ac0af915ef14b7275 3bb9	yes	57				
Multipart Description/PDF files in .zip description									
Document Description		Start		End					
Application Data Sheet		1		1					
Specification		2		54					
Claims		55		56					
Abstract		57		57					
Warnings:									
Information:									
2	Drawings-only black and white line drawings	6460-94 FIGURES.pdf	3532405 b8c151aba653fd22e1248b7edf50f6244582 e514	no	13				
Warnings:									
Information:									
3	Fee Worksheet (PTO-875)	fee-info.pdf	29256 e846da487c2c4f40527071339d5d966b8e8 0c24c	no	2				
Total Files Size (in bytes):				14400500					

This Acknowledgement Receipt evidences receipt on the noted date by the USPTO of the indicated documents, characterized by the applicant, and including page counts, where applicable. It serves as evidence of receipt similar to a Post Card, as described in MPEP 503.

New Applications Under 35 U.S.C. 111

If a new application is being filed and the application includes the necessary components for a filing date (see 37 CFR 1.53(b)-(d) and MPEP 506), a Filing Receipt (37 CFR 1.54) will be issued in due course and the date shown on this Acknowledgement Receipt will establish the filing date of the application.

National Stage of an International Application under 35 U.S.C. 371

If a timely submission to enter the national stage of an international application is compliant with the conditions of 35 U.S.C. 371 and other applicable requirements a Form PCT/DO/EO/903 indicating acceptance of the application as a national stage submission under 35 U.S.C. 371 will be issued in addition to the Filing Receipt, in due course.

New International Application Filed with the USPTO as a Receiving Office

If a new international application is being filed and the international application includes the necessary components for an international filing date (see PCT Article 11 and MPEP 1810), a Notification of the International Application Number and of the International Filing Date (Form PCT/RO/105) will be issued in due course, subject to prescriptions concerning national security, and the date shown on this Acknowledgement Receipt will establish the international filing date of the application.

APPLICATION DATA SHEET

(1) Applicant Information

Inventor (1) name: Cengiz CAMCI
Residence: Boalsburg, Pennsylvania
Mailing Address: 1424 Estate Drive
Boalsburg, Pennsylvania 16827
Citizenship: U.S.A.

Inventor (2) name: Ali AKTURK
Residence: State College, Pennsylvania
Mailing Address: 470 Waupelani Drive
State College, Pennsylvania 16801
Citizenship: TURKEY

(2) Correspondence Information

Correspondence Address: *86002*

(3) Application Information

TITLE: DOUBLE-DUCTED FAN

Total No. of Drawing Sheets: 13
Suggested Figure for Publication: N/A
Docket Number: 6460-94
Type of Application: Provisional Patent

(4) Representative Information

Representative Information: *86002*
Amy A. Dobbelaere, Ph.D., Registration No. 52,088
Novak Druce + Quigg LLP
525 Okeechobee Blvd., 15th Floor
West Palm Beach, FL 33401
Telephone: (561) 847-7800

(5) Domestic Priority Information

N/A

(6) Foreign Priority Information

N/A

(7) Government Funding

Grant No. W911W6-06-2-0008,
U.S. Army Research Office

(8) Assignee Information

Assignee (1) name: Penn State Research Foundation
Assignee address: 113 Technology Center
200 Innovation Boulevard
University Park, Pennsylvania 16802

DOUBLE-DUCTED FAN

FEDERALLY SPONSORED RESEARCH

[0001] The subject matter disclosed herein was developed with government support under grant no. W911W6-06-2-0008 awarded by the U.S. Army Research Office. The U.S. government has certain rights in the invention.

FIELD OF TECHNOLOGY

[0002] The present disclosure relates ducted fans. More specifically, the present disclosure relates to ducted fans for axial-flow rotors.

BACKGROUND

[0003] Axial-flow rotor units include rotating, airfoil-based fans in which the working fluid (e.g., air or other gas) principally flows parallel to the axis of rotation. Axial-flow rotor units are widely used in turbomachinery, such as jet engines, high-speed ship engines, and small-scale power stations. They are also used in industrial applications such as large-volume air separation plants, supplying blast furnace air or fluid catalytic cracking air, and propane dehydrogenation. Additionally, axial-flow rotor units can be used in cooling fans for homes, automobiles, locomotive vehicles, buses, marine vehicles, and aircrafts such as vertical and short take-off and landing (VSTOL) vehicles and uninhabited aerial vehicles.

[0004] In some situations, there can be inlet flow distortion at the inlet of the axial-flow rotor. For example, inlet flow distortion can occur when the inlet flow direction is not well aligned with the axis of rotation of the axial-flow rotor system. In conventional axial-flow ducted fan rotors are often used in VSTOL vehicles to generate the lift force required for hover-type flight. For example, the axial-flow ducted fan rotor can generate a downward-facing force required for hover-type flight. As shown in FIGS. 1A-1C, a conventional ducted fan 1000 includes a hub 100 having a front portion 101 and an end portion 115, a rotor 105 having a

plurality of blades 107 rotatably coupled to the front portion 101 of the hub 100, and a duct 110 surrounding the blades 107 of the rotor 105. In the particular embodiment illustrated, the duct 110 is a cylindrical structure that surrounds the blades 107 of the rotor 105. The duct 110 is coupled to the hub 100 by a plurality of outlet vanes 109. In between the front portion 101 of the hub 100 and the duct 110 is the rotor inlet 125. The rotor inlet 125 includes an inlet lip 119 proximate to the leading edge of the duct 110. The illustrated conventional ducted fan has a single duct. During horizontal flight, cross-wise air flow encounters the outer surface of the duct 110. The cross-wise air flow separates between the top and the bottom of the -duct 110. The air-flow that travels across the leading edge of the duct 110 and past the inlet lip 119 enters the rotor inlet 125. However, as a result of the configuration of the conventional ducted fan, as air-flow enters the rotor inlet 125, there is flow distortion at the inlet lip 119 of the duct 110. This distortion will be referred to herein as inlet-flow separation. The cross-wise air-flow is moved and forced through the rotor inlet 125 by the rotating blades 107 of the rotor 105. The air-flow exits the rotor at the outlet beneath the outlet vanes 109.

[0005] Conventional axial-flow rotor systems moving at 90 degrees angle of attack, with respect to the ground, inherently have an inlet flow direction that significantly deviates from the axis of the rotation of the axial-flow rotor. Thus, because the relative inlet flow is predominantly parallel to the inlet plane of the rotor, problems related to inlet flow separation at the leading edge duct lip 119 are encountered during horizontal flight. The inlet flow separation near the leading side of all of these rotor system inlets becomes more problematic with increasing vehicle speed since the inlet flow distortion passing through a typical axial-flow rotor unit becomes increasingly damaging with elevated forward flight velocity. Furthermore, the lip separation occurring on the inner side of the lip section severely limits the lift generation and controllability of the VSTOL. In general, the leading side of the rotor unit near the lip separation zone breathes poorly when compared to the trailing side of the axial-flow rotor unit. The trailing side total pressure is usually much higher than the total pressure observed near the leading side at the exit of the rotor. The flow near the leading side is negatively influenced by a separated flow zone that is characterized as highly re-circulatory, low-momentum, and turbulent.

[0006] Inlet flow distortion entering into an axial-flow rotor in horizontal flight can cause a number of problems, including the loss of the rotor's ability to add energy to the working fluid near the leading side of the rotor unit; an imbalance in the local mass flow rates between the leading side and trailing side of the rotor unit; an imbalance in the total pressure between the leading side and trailing side at the rotor exit; significant loss of lifting ability due to highly non-axisymmetric and unnecessary rotor unit exit jet flow; and unwanted nose-up pitching-moment generation due to the local static distributions imposed on the rotor unit inner surfaces.

[0007] Therefore, measuring and predicting the mean-flow characteristics of ducted axial-flow rotor systems is crucial to understand the problems related to reliable and controllable horizontal flights. The operation of an axial-flow rotor with strong inlet flow distortion severely affects the performance of the rotor especially near the tip region of the blades of the rotor unit.

BRIEF DESCRIPTION OF THE DRAWINGS

[0008] Various embodiments will now be described, by way of example only, with reference to the attached Figures, wherein:

[0009] FIG. 1A is a perspective view of a conventional ducted fan;

[0010] FIG. 1B is front of the conventional ducted fan illustrated in FIG. 1A;

[0011] FIG. 1C is a vertical cross-section view, taken along lines A-A, of the conventional ducted fan illustrated in FIG. 1A;

[0012] FIG. 2A is a perspective view of an exemplary double-ducted fan in accordance with the technology that is the subject matter of this disclosure;

[0013] FIG. 2B is a front view of the double-ducted fan illustrated in FIG. 2A;

[0014] FIG. 2C is a vertical cross-section view, taken along lines A-A, of the double-ducted fan illustrated in FIG. 2A;

[0015] FIG. 3A is a perspective view of another embodiment of a double-ducted fan in accordance with the technology that is the subject matter of this disclosure, which has a second duct that is shorter than the first duct;

[0016] FIG. 3B is a front view of the double-ducted fan illustrated in FIG. 3A;

[0017] FIG. 3C is a vertical cross-section view, taken along lines A-A, of the double-ducted fan illustrated in FIG. 3A;

[0018] FIG. 4A is a perspective view of another embodiment of a double-ducted fan in accordance with the technology that is the subject matter of this disclosure, which has eccentrically oriented ducts;

[0019] FIG. 4B is a front view of the double-ducted fan illustrated in FIG. 4A;

[0020] FIG. 4C is a vertical cross-section view, taken along lines A-A, of the double-ducted fan illustrated in FIG. 4A; and

[0021] FIG. 5 is a schematic partial cross-section view of the exemplary double-ducted fan illustrated in FIG. 2A illustrating the flow of air across the double-ducted fan.

DETAILED DESCRIPTION

[0022] It will be appreciated that for simplicity and clarity of illustration, where appropriate, reference numerals have been repeated among the different figures to indicate corresponding or analogous elements. In addition, numerous specific details are set forth in order to provide a thorough understanding of the embodiments described herein. However, it will be understood by

those of ordinary skill in the art that the embodiments described herein can be practiced without these specific details. In other instances, methods, procedures and components have not been described in detail so as not to obscure the related relevant feature being described. Also, the description is not to be considered as limiting the scope of the embodiments described herein.

[0023] A double-ducted fan includes a hub, a rotor fan rotatably coupled to the hub, a first duct, and a second duct, wherein the first duct circumscribes the rotor fan and the second duct circumscribes at least a portion of the first duct. The rotor fan has an inlet side and an outlet side. A channel is defined between the first duct and the second duct and is configured to direct air-flow cross-wise to the first duct, over a top of the first duct, into the inlet side of the rotor fan. The second duct is axially oriented upward from the first duct such that there is an axial distance between a leading edge of the first duct and a leading edge of the second duct. In one embodiment the second duct is oriented at an angle with respect to the first duct. In another embodiment, the first duct and the second duct are concentrically oriented. In another embodiment, the first duct and the second duct are eccentrically oriented. In at least one embodiment, the first duct is the inner or intermediate duct, and the second duct is the outer duct. The orientation and configuration of the first duct and second duct of the double-ducted fan reduces and controls the upstream lip separation during operation at high angles of attack. Other configurations and arrangements will be described below in relation to illustrated embodiments. One of ordinary skill will appreciate that the elements from the illustrated embodiments can be optionally included and arranged in various combinations to achieve the described benefits of the presently disclosed double-ducted fan.

[0024] As shown in FIGS. 2A-2C, the double-ducted fan 2000 includes a hub 200 having a front portion 201 and an end portion 215. The end portion 215 of the hub can be the tail cone. A motor and electrical wiring for the double-ducted fan 2000 can be housed in the hub 200 and covered by the tail cone. While the illustrated hub 200 is an elongated structure, one of ordinary skill in the art will appreciate that the hub 200 can be a rotor hub, a rectangular structure, an elliptical structure, a conical structure, or any other aerodynamic structure than can be coupled with a rotor fan 205 and implemented in an axial-flow system.

[0025] A rotor fan 205 having a plurality of blades 207 is rotatably coupled to the front portion 201 of the hub 200. The rotor fan 205 has an inlet side 225 and an outlet or exit side. The double-ducted fan 2000 has a first duct 210 and a second duct 220. In the particular embodiment illustrated, the first duct 210 and the second duct 220 are cylindrical structures. The first duct circumscribes the rotor fan 205. In other words, the first duct 210 is coupled to the rotor 200 such that the first duct 210 surrounds the rotor 205 and is radially spaced from the hub 200. As seen in the illustrated embodiment, the first duct 210 is coupled to the hub 200 at the trailing edge 217 of the first duct 210 by a plurality of outlet vanes 209. The first duct 210 has a leading edge 213, a trailing edge 217, and a first length 255 between the leading edge 213 and the trailing edge 217. An inlet 225 or throat is formed between the first duct 210 and the rotor 200 on an inlet side of the rotor fan 205. Air-flow can enter the rotor fan 205 and pass through the rotor blades 207 to the outlet or exit side of the rotor 205. For example, air can pass from the inlet 225 to the outlet of the rotor fan 205 when the double-ducted fan 2000 is in operation during horizontal motion and while oriented at a 90 degree angle of attack with respect to the ground. The inlet 225 includes an inlet lip 219 proximate to the leading edge 213 of the first duct 210.

[0026] A second duct 220 circumscribes the first duct 210 and can be radially spaced from the first duct 210. The second duct 220 is held in plane by a plurality of struts (not shown) radially attached to the first duct 210. The second duct 220 is coupled to the first duct such that the rotor 205 is at the center of the double-ducted fan 2000. In the illustrated embodiment, the first duct 210 and the second duct 220 are concentric. In at least one embodiment, the second duct 220 is stationary with respect to the first duct 210. As shown in FIG. 2C, the second duct 220 has a leading edge 245, a trailing edge 240, and a second length 250 between the leading edge 245 and the trailing edge 240. For example, in the illustrated embodiment, the second duct 220 has a second length 250 greater than the first length 255 of the first duct 210. In other words, the second duct 220 is longer in length than the first duct 210. Also, as seen in FIG. 2C, the leading edge 245 of the second duct 220 can have a duct lip 247 or an outer lip. Additionally, the leading edge 213 of the first duct 210 has an inlet lip 219.

[0027] The second duct 220 can be oriented axially-upward with respect to the leading edge 213 of first duct 210 as illustrated in FIG. 2C. For example, the second duct 220 can be oriented such that the leading edge 245 of the second duct 220 is oriented axially-upward from the leading edge 213 of the first duct 210. In other words, the leading edge 245 of the second duct 220 is located forward and upward from the leading edge 213 of the first duct 210. As illustrated in FIG. 2C, the second duct 220 has a second length 250 longer than the first length 255 of the first duct 210. The trailing edge 250 of the second duct 220 and the trailing edge 217 of the first duct 210 are axially aligned so that there is an axial distance 260 between the leading edge 245 of the second duct and the leading edge 213 of the first duct 210. A channel 230 is formed between the first duct 210 and the second duct 220. As illustrated in FIG. 2C, the channel 230 can be a converging-diverging channel. For example, the width 275 of the channel 230 can vary from the trailing edges 217, 240 of the first and second ducts 210 and 220, to the leading edges 213, 245 of the first and second duct 210, 220 (e.g., the width 275 can increase or decrease). As the first duct 210 and the second duct 220 are concentric, the shape of the converging-diverging channel 230 does not vary circumferentially around the rotor 200. Also as shown in FIG. 2C, the first duct 210 and the second duct 220 have an airfoil shape. However, in alternative embodiments, the first duct 210 and the second duct 220 can have a circular shape, a cylindrical shape, an oval shape, or any other shape that permits air flow into the inlet 225 of the rotor 205.

[0028] In the embodiment illustrated in FIGS. 2A-2C, during horizontal flight, cross-wise air-flow will encounter the second duct 220 (e.g. air-flow will move from the left to the right in FIG. 2C). As the cross-wise air-flow encounters the duct lip 247, a portion of the air-flow will travel upwards towards the leading edge 245 of the second duct 220, and a portion of the air-flow will travel downwards towards the trailing edge 240 of the second duct 220. The air-flow that travels across the leading edge 245 will flow across the leading edge 213 of the first duct 210, over the inlet lip 219, and into the rotor inlet 225. The air-flow that travels towards the trailing edge 240 of the second duct 220 will travel upwards through the channel 230, over the leading edge 213 of the first duct 210 and the inlet lip 219, and into the rotor inlet 225. Because the air-flow encounters the second duct 220 first during horizontal flight, the air-flow is separated at the

second duct 220 before it encounters the inlet lip 219 of the first duct 210. Thus, the air-flow entering the rotor inlet 225 is substantially uniform, and the inlet separation that would typically occur in conventional ducted fans is reduced. As a more uniform air-flow profile enters the rotor inlet 225, more uniform air-flow exits the rotor 205, thereby reducing energy loss, total pressure imbalance, and mass-flow rate imbalance that can be associated with air-flow distortion.

[0029] As shown in FIGS. 3A-3C, another embodiment of the double-ducted fan 3000 includes a hub 300 having a front portion 301 and an end portion 315. A rotor fan 305 having a plurality of blades 307 is rotatably coupled to the front portion 301 of the hub 300. A first duct 310 is coupled to the rotor 300 such that the first duct 310 surrounds the rotor 305 and is radially spaced from the hub 300. The first duct 310 has a leading edge 313, a trailing edge 317, and a first length 355 between the leading edge 313 and the trailing edge 317. As seen in the illustrated embodiment, the first duct 310 is coupled to the hub 300 at the trailing edge 317 of the first duct 310 by a plurality of outlet vanes 309. An inlet 325 is formed between the first duct 310 and the rotor 300 through which air-flow can pass when the double-ducted fan 3000 is in operation during horizontal motion and while oriented at a 90 degree angle of attack with respect to the ground. The inlet 325 includes an inlet lip 319 proximate to the leading edge 313 of the first duct 310.

[0030] A second duct 320 is radially spaced from the first duct. The second duct 320 is held in plane by a plurality of struts (not shown) radially attached to the first duct 310. The second duct 320 is coupled to the first duct such that the rotor 305 is at the center of the double-ducted fan 3000. In the illustrated embodiment, the first duct 310 and the second duct 320 are concentric with the second duct 320 is stationary with respect to the first duct 310. In the illustrated embodiment, the first duct 310 and the second duct 320 are cylindrical structures; however, one of ordinary skill in the art will appreciate that the first duct 310 and second duct 320 can be any structure that permit axial air-flow into the inlet 325 of the rotor fan 305.

[0031] As shown in FIG. 3C, the second duct 320 has a leading edge 345, a trailing edge 350, and a second length 350 between the leading edge 345 and the trailing edge 340. For example,

in the illustrated embodiment, the second duct 320 has a second length 350 so that the second duct 320 is shorter than the first duct 310. In comparison to the embodiment shown in FIGS. 2A-2C, the embodiment illustrated in FIGS. 3A-3C has a second duct 320 that is shorter than the first duct 310.

[0032] As illustrated in FIG. 3C, the second duct 320 is oriented axially-upward with respect to the first duct 310. For example, the second duct 320 is oriented such that the leading edge 335 of the second duct 320 is oriented axially-upward from the leading edge 313 of the first duct 310. In other words, the leading edge 345 of the second duct 320 is located forward and upward from the leading edge 313 of the first duct 310. Additionally, the trailing edge 350 of the second duct 320 and the trailing edge 317 of the first duct 310 are axially aligned so that there is an axial distance 360 between the leading edge 345 of the second duct and the leading edge 313 of the first duct 310. A channel 330 is formed by the first duct 310 and the second duct 320. As illustrated in FIG. 3C, the channel 330 can be a converging-diverging channel. For example, the width 375 of the channel 330 can vary from between the trailing edges 317, 340 of the first and second ducts 310, 320 to the leading edges 313, 345 of the first and second duct 310, 320 (e.g., the width 375 can increase or decrease). As the first duct 310 and the second duct 320 are concentric, the converging-diverging channel 330 does not vary circumferentially around the rotor 300. Also as shown in FIG. 3C, the first duct 310 and the second duct 320 have an airfoil shape. However, in alternative embodiments, the first duct 310 and the second duct 320 can have a cylindrical shape, an oval shape, or any other shape that permits axial air flow into the inlet 345 of the rotor 305.

[0033] Similar to the embodiment illustrated in FIGS. 2A-2C, for the embodiment illustrated in FIGS. 3A-3C, during horizontal flight, cross-wise air-flow will encounter the second duct 320 before it encounters the leading edge 313 of the first duct 310 (e.g., air-flow will move from the left to the right in FIG. 3C). As the cross-wise air-flow encounters the duct lip 347, a portion of the air-flow will travel upwards towards the leading edge 345 of the second duct 320, and a portion of the air-flow will travel downwards towards the trailing edge 340 of the second duct 320. The air-flow that travels across the leading edge 345 will flow across the leading edge 313 of the first duct 310, over the inlet lip 319, and into the rotor inlet 325. The air-flow that travels

towards the trailing edge 340 of the second duct 320 will travel upwards through the channel 330, over the leading edge 313 of the first duct 310 and the inlet lip 319, and into the rotor inlet 325. Compared to the embodiment illustrated in FIG. 2C, as a result of the shorter second duct 320, the air-flow at the trailing edge 340 is further directed upward into the channel 330 by the trailing edge 317 of the first duct 310. Because the air-flow encounters the second duct 320 first during horizontal flight, the air-flow is separated at the second duct 320 before it encounters the inlet lip 319 of the first duct 310. Thus, the air-flow entering the rotor inlet 325 is substantially uniform, and the inlet separation that would typically occur in conventional ducted fans is reduced. As a more uniform air-flow profile enters the rotor inlet 325, more uniform air-flow exits the rotor 305, thereby reducing energy loss, total pressure imbalance, and mass-flow rate imbalance that can be associated with air-flow distortion.

[0034] As shown in FIGS. 4A-4C, another embodiment of the double-ducted fan 4000 includes a hub 400 having a front portion 420 and an end portion 415. A rotor fan 405 having a plurality of blades 407 is rotatably coupled to the front portion 401 of the hub 400. A first duct 410 is coupled to the rotor fan 405 such that the first duct 410 surrounds the rotor fan 405 and is radially spaced from the hub 400. The first duct 410 has a leading edge 413, a trailing edge 417, and a first length 455 between the leading edge 413 and the trailing edge 417. As shown in the illustrated embodiment, the first duct 410 is coupled to the hub 400 at the trailing edge 417 of the first duct 410 by a plurality of outlet vanes 409. An inlet 425 or throat is formed between the first duct 410 and the rotor 400 through which air flow can pass when the double-ducted fan 4000 is in operation during horizontal motion and while oriented at a 90 degree angle of attack with respect to the ground. The inlet 425 includes an inlet lip 419 proximate to the leading edge 413 of the first duct 410.

[0035] A second duct 420 is radially spaced from the first duct. The second duct 420 is coupled to the first duct such that the rotor 405 is at the center of the double-ducted fan 4000. The second duct 420 has a leading edge 445, a trailing edge 450, and a second length 450 between the leading edge 445 and the trailing edge 440. For example, as illustrated in FIG. 4C, the second duct 420 has a second length 450 is shorter in than the first length 455 of the first duct

410. However, in at least one alternative embodiment, the second duct 420 can have a second length 450 longer than the first length 455 of the first duct 410. In the illustrated embodiment, the first duct 410 and the second duct 420 are cylindrical structures; however, one of ordinary skill in the art will appreciate the first duct 410 and the second duct 420 can be any structure that will direct cross-wise air-flow into the inlet 425 of the rotor fan 405.

[0036] As compared to the embodiment illustrated in FIGS. 2A-3C, the illustrated embodiment of FIGS. 4A-4C show the first duct 410 and the second duct 420 eccentrically oriented. As illustrated in FIG. 4C, the second duct 420 is oriented axially-upward with respect to the first duct 410. For example, the second duct 420 is oriented such that the leading edge 445 of the second duct 420 is oriented axially-upward from the leading edge 413 of the first duct 410. The trailing edge 450 of the second duct 420 and the trailing edge 417 of the first duct 410 are aligned such that there is an axial distance 460 between the leading edge 445 of the second duct and the leading edge 413 of the first duct 410. A channel 430 is formed between the first duct 410 and the second duct 420. As illustrated in FIG. 4C, the channel 430 is a converging-diverging channel. For example, the width 405 of the channel 430 can vary from the trailing edges 417, 440 of the first and second ducts 410, 420 to the leading edges 413, 435 of the first and second duct 410, 420 (e.g., the width 475 can increase or decrease). As the first duct 410 and the second duct 420 are eccentric, the width 405 and shape of the converging-diverging channel 430 can vary circumferentially around the rotor 400. For example, the width 475 of the portion of the converging-diverging channel 430 where the first duct 410 is closest to the inner wall of the second duct 420 (the width 475 to the left of the central axis 465 in FIG. 4C) is smaller than the width of the portion of the converging-diverging channel 400 where the first duct 410 is further from the inner wall of the second duct 420 (the width 475 to the right of the central axis 465 in FIG. 4C). With the embodiment illustrated in FIGS. 4A-4C, the second duct 420 can be movable with respect to the first duct 410 and the hub 400. Also as shown in FIG. 4C, the first duct 410 and the second duct 420 have an airfoil shape. However, in alternative embodiments, the first duct 410 and the second duct 420 can have a cylindrical shape, an oval shape, or any other shape that permits axial air flow into the inlet 445 of the rotor 405.

[0037] Similar to the embodiment illustrated in FIGS. 2A-3C, for the embodiment illustrated in FIGS. 4A-4C, during horizontal flight, cross-wise air-flow will encounter the second duct 420 before it encounters the leading edge 413 of the first duct 410 (e.g., air-flow will move from the left to right in FIG. 4C). However, unlike the embodiments illustrated in FIGS. 2A-3C, the embodiment illustrated in FIGS. 4A-4C permits a converging-diverging channel 430 that can vary depending on the angle of attack which the double-ducted fan 4000 is oriented. As the cross-wise air-flow encounters the duct lip 447, a portion of the air-flow will travel upwards towards the leading edge 445 of the second duct 420, and a portion of the air-flow will travel downwards towards the trailing edge 340 of the second duct 420. The air-flow that travels across the leading edge 445 will flow across the leading edge 413 of the first duct 410, over the inlet lip 419, and into the rotor inlet 425. The air-flow that travels towards the trailing edge 440 of the second duct 420 will travel upwards through the channel 430, over the leading edge 413 of the first duct 410 and the inlet lip 419, and into the rotor inlet 425. Compared to the embodiments illustrated in FIG. 2C and 3C, as a result of the eccentric first duct 410 and second duct 420, the channel 430 can be opened or closed to permit air-flow at the trailing edge 440 of the second duct 420 to be directed upward into the channel 430 and over and into the rotor inlet 425. Adjusting the width 475 of the converging-diverging channel 430 allows for more controlled air-flow into the rotor inlet 425. Because the air-flow encounters the second duct 420 first during horizontal flight, the air-flow is separated at the second duct 420 before it encounters the inlet lip 419 of the first duct 410. Thus, the air-flow entering the rotor inlet 425 is substantially uniform, and the inlet separation that would typically occur in conventional ducted fans is reduced. As a more uniform air-flow profile enters the rotor inlet 425, more uniform air-flow exits the rotor fan 405, thereby reducing energy loss, total pressure imbalance, and mass-flow rate imbalance that can be associated with air-flow distortion.

[0038] The movement of air flow through the double-ducted fan as illustrated in any of the previously described embodiments will now be described. For purposes of brevity, the movement of air through the double-ducted fan will be described with respect to the illustrated embodiment in FIG. 5, which illustrates a double-ducted fan 5000 having a second duct 520

shorter than the first duct 510. FIG. 5 is a partial vertical cross-section view of an exemplary double-ducted fan 5000 in accordance with an exemplary embodiment. In particular, FIG. 5 is a vertical cross-section view the left side of the double-ducted fan 5000 with respect to the central axis 565. As illustrated in FIG. 5, the double-ducted fan 5000 includes a hub 500, a rotor (not shown) having a plurality of blades rotatably coupled to the hub 500, a first duct 510 axially spaced from the hub 5000 and surrounding the rotor, and a second duct 520 axially spaced from the first duct 510. An inlet 525 or throat is formed between the first duct 510 and the hub 500 which permits air flow to pass from the atmosphere through the blades of the rotor. The illustrated embodiment in FIG. 5 shows the second duct 520 have a length 550 shorter than the length 555 of the first duct 510. Additionally, the second duct 220 is oriented axially upward from the leading edge 513 of the first duct 510 such that the leading edge 535 of the second duct 520 is spaced an axial distance 560 from the leading edge 513 of the first duct 510. The second duct 520 has the cross-section of an air foil and is oriented at an angle with respect to the first duct 510. In the illustrated example, the second duct 520 is cambered away from the first duct 510 and with respect to the central axis 565 of the double-ducted fan 5000.

[0039] A channel 530 is formed between the second duct 520 and the first duct 510. In the particular embodiment illustrated in FIG. 5, the channel 530 is a converging-diverging channel whereby the width 575 of the channel 530 decreases from between the leading edges 513, 535 of the first duct 510 and the second duct 520 to between the trailing edges 517, 540 of the first duct 510 and the second duct 520. During operation in forward flight in which the double-ducted fan 5000 is oriented at a 90 degree angle of attack with respect to the ground, horizontal or cross-wise air flow (depicted as 5100) encounters the second duct 520. In the illustrated embodiment, air flow moves from the leading side of the double-ducted fan 5000, which is to the left of the central axis 565, to the trailing side (not shown) of the double-ducted fan, which is to the left of the central axis 565. The flow in the channel 530 is directed from the trailing edge 517 to the leading edge 513 of the first duct 510. In other words, the upward flow feature in the channel 530 belongs to a local region around the leading side of the second duct 520. When moving away from the leading side of the second duct 520, air-flow in the channel 530 is directed from top to below which is the same overall flow direction in rotor inlet 525. As a result of the orientation

and shapes of the first duct 510 and the second duct 520, the horizontal air flow is directed upward through the channel 530, over the first duct 510, and downward into the inlet 525 of the rotor. The upward flow direction through the channel 530 and the downward flow into and through the inlet 525 provides for controlled inlet flow distortion and a reduced air flow separation near the inlet lip 519 of the leading side (the left side of the illustrated embodiment) of the double-ducted fan 5000. For example, since the cross-wise air flow encounters the leading edge 545 of the second duct 520, more uniform air-flow travels across the leading edges 545, 513 of the second duct 520 and the first duct 510. The inlet separation at the inlet lip 519 is thereby reduced allowing for less distorted air-flow that enters the rotor inlet 525. Additionally, the orientation and shapes of the first duct 510 and second duct 520 enhance the uniformity of rotor fan exit flow and reduce differentials between the leading side and trailing side of the double-ducted fan 5000. For example, because the portion of air-flow that is directed upwards through the channel 530 meets the portion of air-flow that travels across the leading edge 545 of the second duct 520, the air-flow is uniform as it travels across the leading edge 513 of the first duct 510. As a result, air flow from the rotor 500 at the exit or outlet of the rotor 500 can provide a thrust force to enhance the performance of the vehicle to which the double-ducted fan 5000 is coupled. Furthermore, the resulting shape of the double-ducted fan 5000 due to the orientation and shape of the first duct 510 and second duct 520 can reduce drag during forward flight. With any of the exemplary embodiments of the double-ducted fan described herein, the orientation and shape of the first duct and second duct can reduce the inlet lip separation or air flow separation at the inlet lip associated with conventional axial-flow rotor units, enhance the exit air flow of the ducted fan, enhance the thrust force of the ducted fan, and control inlet flow distortion that can be associated with conventional axial-flow rotor units.

[0040] The following figures illustrate a double-ducted fan per the subject technology. While the illustrated embodiments are particularly suited for a vertical or short-take-off-and-landing vehicle (VSTOL), one of ordinary skill in the art will appreciate that the double-ducted fan described could be implemented in an uninhabited aerial vehicle; a cooling fan for a train; a passenger bus; a marine vehicle; or any other vehicle that uses an axial-flow rotor unit. Additionally, the double-ducted fan could be implemented in any axial flow fan unit where there

is an inlet flow distortion due to the inlet flow direction not being well-aligned with the axis of rotation of the axial fan unit. An appendix follows describing in details regarding the experimentation and testing results of the various embodiments of the double-ducted fan described herein. Various modifications to and departures from the disclosed embodiments will occur to those having skill in the art. The subject matter that is intended to be within the spirit of this disclosure is set forth in the following claims.

APPENDIX

A

APPENDIX – Exemplary Studies of the Double Ducted Fan

A ducted fan inlet flow conditioning concept that can enhance the performance and controllability of V/STOL “vertical/short take off take-off and landing” UAVs “uninhabited aerial vehicles” and many other ducted fan based systems. The new concept that can reduce the inlet lip separation related performance penalties in the forward flight zone is named “DOUBLE DUCTED FAN” (DDF). The current concept uses a secondary stationary duct system to control “inlet lip separation” related momentum deficit at the inlet of the fan rotor occurring at elevated forward flight velocities. The DDF is self-adjusting in a wide forward flight velocity range. DDFs corrective aerodynamic influence becomes more pronounced with increasing flight velocity due to its inherent design properties. The DDF can also be implemented as a “Variable Double Ducted Fan” (VDDF) for a much more effective inlet lip separation control in a wide range of horizontal flight velocities in UAVs, air vehicles, trains, buses, marine vehicles and any axial flow fan system where there is a local zone in which there are strong radial velocity components distorting the inlet flow. Most axial flow fans are designed for an inlet flow with zero or minimal inlet flow distortion. The DDF concept is proven to be an effective way of dealing with inlet flow distortions occurring near the lip section of any axial flow fan rotor system.

Nomenclature

β_1, β_2	= Blade inlet, exit angle measured from axial direction
c	= Axial chord of the standard duct
c_1, c_2	= Rotor inlet, exit absolute velocity
c_o	= Tangential (swirl) velocity component
c_x	= Axial velocity
D	= Overall diameter of the baseline ducted fan
h	= Rotor blade height
p	= Static Pressure
P_o	= Total Pressure
Ω	= Rotational Speed (radian/sec)
r	= Radial distance measured from origin
t	= Rotor tip clearance
w_1, w_2	= Rotor inlet, exit relative velocity (also W)
X	= Axial coordinate measured from the inlet plane of the standard duct
x	= X/c , non-dimensional axial distance
ρ	= Density

Although there is a strong interest in V/STOL UAV community to effectively deal with the upstream lip separation problem of ducted fans, the inlet flow distortion problem is common to many present day fan rotors in a wide variety of applications. The current conceptual design study clearly shows that the DDF approach is applicable to any axial flow fan unit in which there is an inlet flow distortion mainly because the inlet flow

direction is not well aligned with the axis of rotation of the axial fan system. A few other examples that will easily benefit from the DDF concept described in this document are the cooling fans that are horizontally mounted at the roof of electric/diesel train locomotive propulsion cabins, air conditioning fans frequently installed at the roofs of passenger buses and cooling/utility fans that are flush mounted to external surfaces in marine vehicles.

A conventional baseline duct without any lip separation control feature is compared to two different double ducted fans named DDF-A and DDF-B via 3D, viscous and turbulent flow analysis. Both hover and forward flight conditions are considered. Enhancements from DDF-A and DDF-B are in the areas of vertical force (thrust) enhancement, nose-up pitching moment control and recovery of mass flow rate in a wide horizontal flight range. The results also show a major reduction of highly 3D and re-circulatory inlet lip separation zone when the DDF concept is implemented. The enhanced uniformity of fan exit flow and reduced differentials between the leading side and trailing side are obvious performance enhancing features of the double ducted concept. The local details of the flow near the entrance area of the leading side of the ducted fan are explained via detailed static pressure distributions and skin friction coefficients obtained from 3D viscous and turbulent flow analysis including a simulated rotor in the duct.

Upstream lip region flow physics for ducted fans in forward flight: Conventional ducted fan systems horizontally moving at 90 degree angle of attack all inherently have an inlet flow direction that deviates from the axis of the rotation. The inlet flow distortion near the leading side of all of these fan inlets becomes more problematic with increasing vehicle speed. The inlet flow distortion passing through a typical axial flow fan rotor becomes increasingly damaging with elevated forward flight velocity. The lip separation occurring on the inner side of the lip section severely limits the lift generation and controllability of V/STOL UAVs. In general, the leading side of the fan near the lip separation zone breathes poorly when compared to the trailing side of the ducted fan. The trailing side total pressure is usually much higher than the total pressure observed near the leading side at the exit of the rotor. The flow near the leading side is negatively influenced by a separated flow zone that is characterized as highly re-circulatory, low momentum and turbulent.

Conventional ducted fan systems also have a tip clearance loss that is proportional with the effective tip gap inherent to each design. The specific shape of the tip platform and the surface properties and arrangement designed onto the casing surface also influences the magnitude of tip clearance loss. This aerodynamic deficiency is measured as a total pressure loss near the tip at the exit of the rotor all around the circumference when the vehicle is only hovering with no horizontal flight. When the vehicle transits into a horizontal flight zone, the total pressure loss/deficit at the exit of the rotor near the leading side is much more significant than "hover only" loss of the ducted fan. In

addition to the conventional tip clearance energy loss, the rotor generates additional losses near the leading side, because of the re-circulatory low momentum fluid entering into the rotor near the tip section. This is clearly an off-design condition for an axial flow fan that is designed for a reasonably uniform inlet axial velocity profile in the spanwise direction. The immediate results of any inlet flow distortion entering into an axial fan rotor in horizontal flight are the loss of rotor's energy addition capability to the fluid near the leading side, an imbalance of the local mass flow rates between the leading side and trailing side, an imbalance of the total pressure resulting at the rotor exit between the leading side and trailing side, a loss of lifting ability due to highly non-axisymmetric and unnecessarily 3D fan exit jet flow, unwanted nose-up pitching moment generation because the local static distributions imposed on the duct inner surfaces.

Conventional ducted fans that have been implemented in V/STOL uninhabited aerial vehicles (UAV) have offered a higher static thrust/power ratio for a given diameter than open propellers. They also provide an impact protection for the blades and enhanced personnel safety due to its enclosed fan structure as well as the lower noise level in the plane of the rotating fan blade.

The viscous flow characteristics of the ducted fan are complex. These vehicles need to be capable of flight in a broad range of atmospheric conditions, including the complex turbulent flow fields around buildings and trees. When a V/STOL ducted fan is in horizontal flight, because of the relative inlet flow dominantly parallel to its inlet plane, problems related to flow separation at the leading edge duct lip are encountered. The inlet flow separation leads to problems within the duct and may well result in a high nose-up pitching moment as the forward speed is increased. Therefore, measuring and predicting the mean flow characteristics of ducted fans is crucial to understand the problems related to reliable and controllable horizontal flights. Numerous studies have been undertaken in order to quantify the flow field characteristics around ducted fans. The operation of an axial flow fan with strong inlet flow distortion severely affects the performance of the rotor especially near the tip region of the blades.

Lip separation at high angle of attack: The "double-ducted Fan (DDF) is based on a very effective fluid mechanics scheme of reducing and controlling the upstream lip separation in a ducted fan operating at high angle of attack. Early research results clearly demonstrating the limits of onset of upstream lip separation in function of angle of attack are summarized in Figure A. A full scale duplicate of the V/STOL ducted propeller used on the Bell Aerosystems Co. X-22A airplane was tested in Ames Research center by Mort and Gamse¹¹. Stall of both the upstream and downstream duct lips of this seven foot diameter ducted fan was examined in function

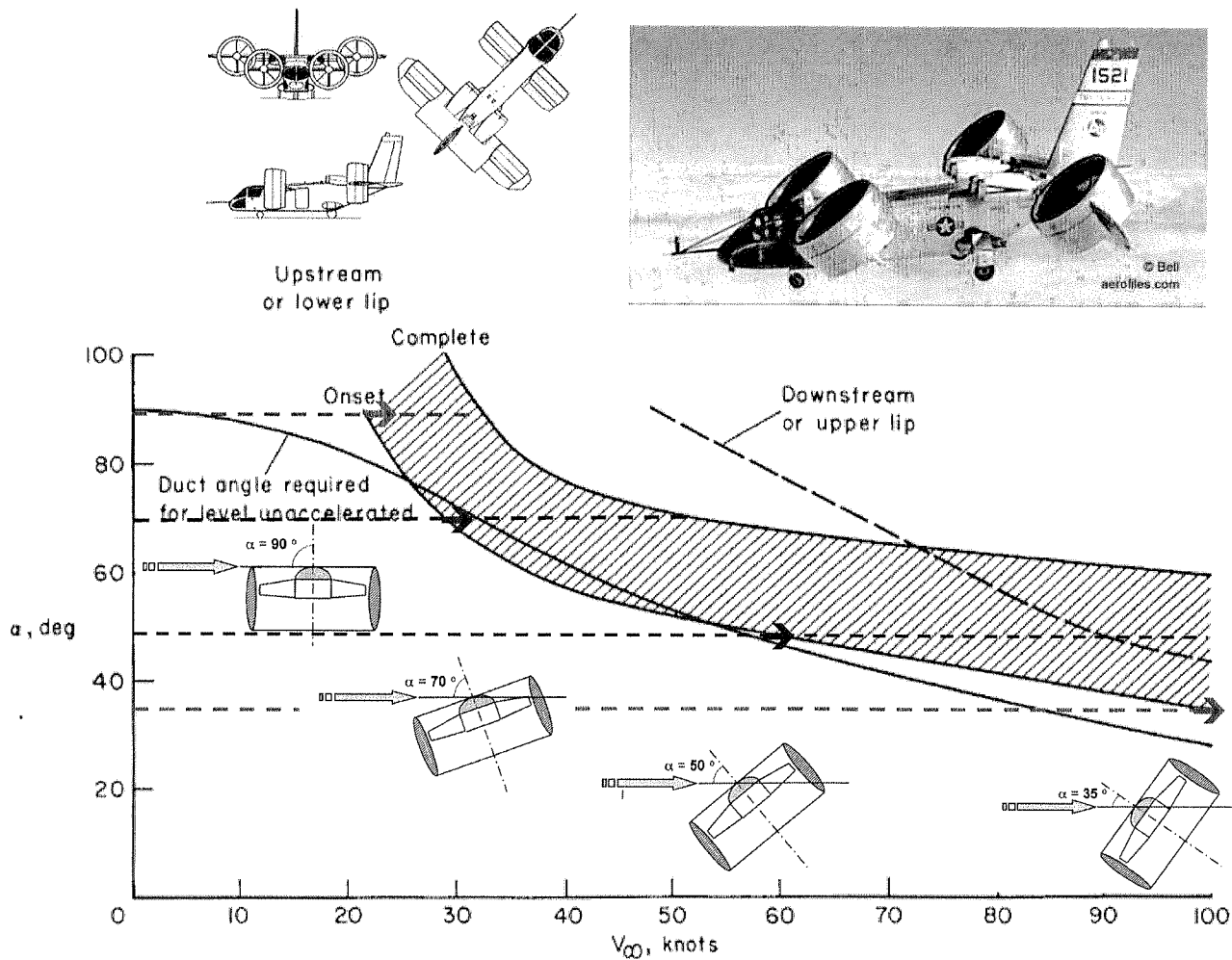


Figure A. Upstream duct lip stall in function of angle of attack for X-22A ducted fan, Mort and Gamse

of angle of attack. The angle of attack of the ducted fan is measured between the approaching flow direction and the axis of rotation of the rotor. It was found that the onset of separation on the upstream lip will be encountered; however, complete separation on this lip will be encountered only during conditions of low power and high duct angle of attack corresponding to high rates of descent.

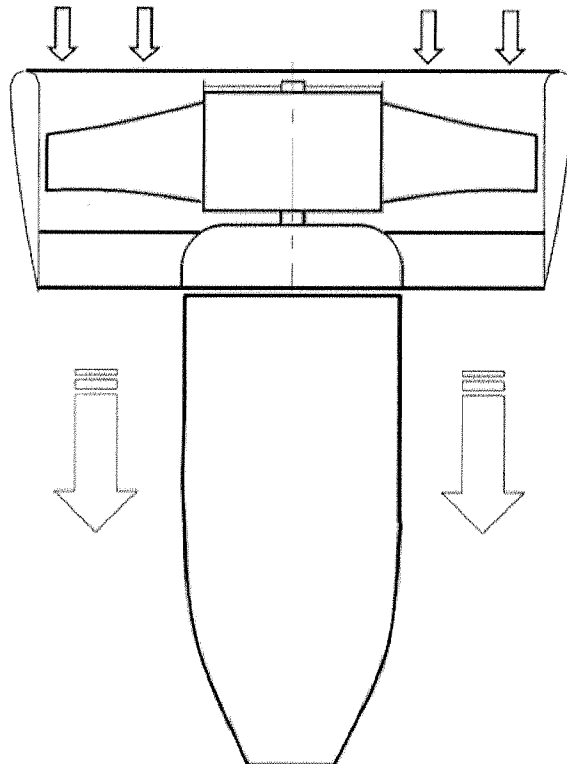
At large duct angles of attack, the inside of the upstream duct lip stalled causing a rapid change in the duct pitching moments and accompanying increase in the power required. At low horizontal velocities this lip stall would probably limit the rate of descent of a vehicle with a wing tip mounted ducted fan. The wind tunnel test results shown in Figure A are highly relevant in demonstrating the beneficial aerodynamic characteristics of the double ducted fan DDF concept presented in this paper.

Adverse effects of upstream lip separation in forward flight: At high angle of attacks, the onset separation at the upstream duct lip is accompanied by the formation of a separation bubble. Existence of a separation bubble can distort inlet flow of the fan rotor especially near the leading side and in the tip clearance region. Distorted inlet flow causes an asymmetric loading of the ducted fan which increases the power required for level un-accelerated flight and noise level. The immediate results of operating a ducted fan in horizontal flight regime especially at high angle of attack are as follows:

- ⇒ Increased aerodynamic losses and temporal instability of the fan rotor flow when "inlet flow distortion" from "the lip separation area" finds its way into the tip clearance gap leading to the loss of "energy addition capability" of the rotor .
- ⇒ Reduced thrust generation from the upstream side of the duct due to the rotor breathing low-momentum, re-circulatory, turbulent flow.
- ⇒ A severe imbalance of the duct inner static pressure field resulting from low momentum fluid entering into the rotor on the leading side and high momentum fluid unnecessarily energized near the trailing side of the rotor.
- ⇒ A measurable increase in power demand and fuel consumption when the lip separation occurs to keep up with a given operational task.
- ⇒ Lip separation and its interaction with the tip gap flow requires a much more complex vehicle control system because of the severe non-uniformity of the exit jet in circumferential direction and excessive nose-up pitching moment generation .
- ⇒ At low horizontal speeds a severe limitation in the rate of descent and vehicle controllability may occur because of more pronounced lip separation. Low power requirement of a typical descent results in a lower disk loading and more pronounced lip separation.
- ⇒ Excessive noise and vibration from the rotor working with a inlet flow distortion.
- ⇒ Very complex unsteady interactions of duct exit flow with control surfaces.

REFERENCE DUCTED FAN CHARACTERISTICS

Figure B shows a five bladed reference conventional ducted fan that is used. The relatively poor forward flight characteristics of the reference ducted fan shown in Figure B are enhanced via the new double ducted fan (DDF) concept that is explained in the next few paragraphs. The geometric specifications of the reference ducted fan unit that is designed for small scale uninhabited aircraft are presented in the accompanying table. This unit is manufactured from carbon composite material and has six vanes at the exit of the fan in order to remove some of the swirl existing at the exit of the rotor. A tail cone is used to cover the motor surface and hide the electrical wiring. All computational 3D flow simulations of the reference duct including the rotor flow field are performed using the geometry defined in Figure B at 9000 rpm.



Rotor hub diameter	52 mm
Rotor tip diameter	120
Duct inner diameter	126
Blade height h	34
Tip clearance t/h	8.7 %
Max. blade thickness @ tip	1.5
Tailcone diameter	52
Tailcone length	105

	HUB	MID SPAN	TIP
Blade inlet angle β_1	60°	40°	30°
Blade exit angle β_2	30°	45°	60°
Blade chord mm	32	30	28
Tip Mach number	$\Omega \cdot r_{tip} / \sqrt{\gamma R T_\infty}$		0.28
Reynolds number (mid-span)	$\rho W_m c / \mu$		7×10^4

Figure B. Reference ducted fan characteristics

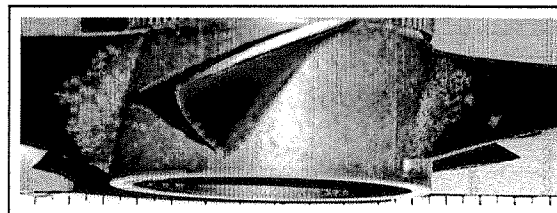


Figure C. Reference ducted fan rotor (five bladed)

Although, the reference ducted fan rotor had a tip clearance of $t/h=8.7\%$, the tip clearance influence on the rotor downstream flow was knowingly excluded from the current 3D computational flow effort. The present simplified rotor flow model does not include tip clearance effects since the current effort is focused on the accurate simulation of the lip separation flow during forward flight of the vehicle.

DOUBLE DUCTED FAN (DDF)

Operational character of the DDF: A double ducted fan concept over a standard ducted fan is explained in Figure D. The poor forward flight characteristics of the reference duct as shown in Figure D(a) are effectively

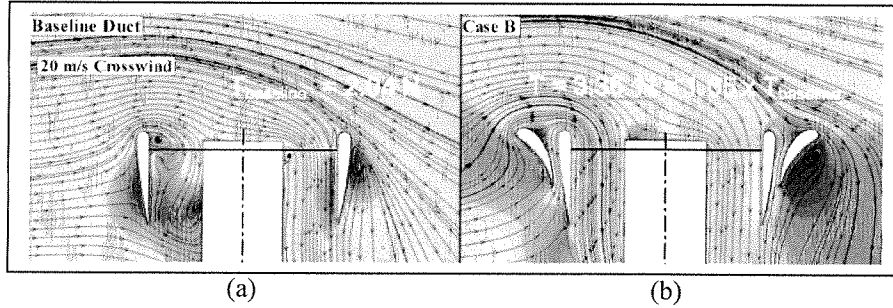


Figure D. Separated flow near the forward lip section of a standard ducted fan (left) and the flow enhancements from the Double Ducted Fan (DDF) at 9000 rpm, colored by the magnitude of velocity (Red/high, Green/intermediate, Blue/low)

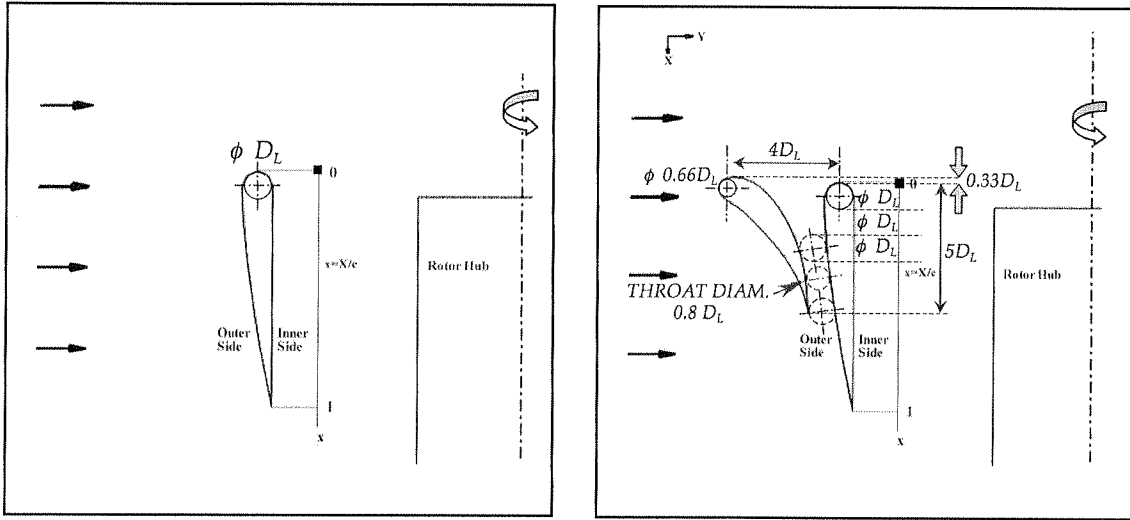


Figure E(a) Reference duct airfoil definition in a standard ducted fan arrangement

Figure E(b) Double Ducted Fan (DDF) geometry

enhanced with the "Double Ducted Fan" concept as presented in Figure D(b). A typical deficiency of a standard ducted fan is mainly related to the forward lip separation

increasingly occurring when the forward flight velocity is gradually increased as shown in the streamline patterns of Figure D(a). The inlet flow near the leading side of the standard duct is highly separated, low-momentum and turbulent. The apparent flow imbalance between the leading side and trailing side of the standard ducted fan shown in Figure D(a) is also called an “inlet-flow-distortion”. Flow simulations in Figure D(a) show that the rotor barely breathes at the inlet section of the leading side although the trailing side passes an amount of flow. This flow imbalance amplified during the rotor “energy adding process” is one of the reasons of nose-up pitching moment generation. Figure D(b) also presents the Double Ducted Fan (DDF) flow simulations indicating the effective inlet flow distortion reduction due to the unique aerodynamic properties of the (DDF) system. The upstream lip separation near the leading side is almost eliminated resulting in a more balanced rotor exit flow field between the leading side and the trailing side. More detailed descriptions of the local flow field enhancements resulting from the Double Ducted Fan (DDF) concept are discussed in the final part of this document. Although there may be many other potentially beneficial variations of the Double Ducted Fan concept, only the specific (DDF) form defined in Figure E(b) will be explained in detail in the preceding paragraphs.

Geometrical definition of DDF: The DDF concept uses a second duct using a lip airfoil shape that has a much shorter axial chord length than that of the standard duct. The key parameter in obtaining an effective DDF arrangement is the size of the lip diameter D_L of the standard ducted fan. The second duct airfoil that is relatively cambered has a leading edge diameter set to $0.66D_L$ as explained in Figure E(b). The angular orientation and axial position of the second duct airfoil is extremely important in achieving a good level of flow enhancement near the leading side of the rotor. The leading edge circle of the second duct airfoil is slightly shifted up in the vertical direction for proper inlet lip separation control. The vertical distance between the duct inlet plane touching the standard duct and the plane touching the second duct is about $0.33D_L$ as shown in Figure E(b). The horizontal distance between the centers of the leading edge circles of the standard duct and outer duct is about $4D_L$. The axial chord of the second duct airfoil is about $5D_L$. The separation distance between the standard duct and second duct is controlled by the recommended throat width of $0.8D_L$ as shown in Figure E(b).

Figure F presents exemplary dimensions of the double ducted fan CASE-B described in the present study. The leading edge diameter $D_L=8.5\text{ mm}$ (0.3 inch) and the axial chord of the standard duct is $c= 58.6\text{ mm}$ (2.31 inch). The general DDF design philosophy described in this section could easily be applied to obtain many other DDF geometries depending upon the vehicle size, rotor diameter, rotor disk loading and forward flight velocity range.

Converging-diverging channel in the duct: The second duct and the standard duct forms a converging-diverging channel starting from the trailing edge of the second

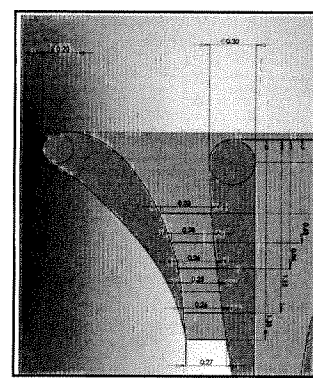


Figure F. Exemplary dimensions of the Double Ducted Fan (in inches)

(outer) duct that is located at about $X=5D_L$. The axial position of the throat section is about $0.45c$ where c is the axial chord of the inner duct as shown in Figure E(b). The duct width at the entrance of the converging-diverging duct is D_L . The entrance to the converging-diverging channel is at the trailing edge point of the second duct. There is a (vertically up) net flow in the converging-diverging duct of the DDF. This flow is due to increasing dynamic pressure at the entrance of the converging-diverging duct at $X=5D_L$ when the forward flight velocity is increased. The diverging part of the channel flow between the standard and outer duct is extremely important in this concept, since this decelerating flow is instrumental in adjusting the wall static pressure gradient just before the lip section of the leading edge of the standard duct. The self-adjusting dynamic pressure of the inlet flow into the converging-diverging duct is directly proportional with the square of the forward flight velocity of the vehicle. The converging-diverging duct flow is in vertically up direction near the leading edge of the vehicle. The flow in the intermediate channel is vertically down when one moves away from the frontal section of the vehicle. This flow direction is caused by the relatively low stagnation pressure at the inlet of the intermediate channel at circumferential positions away from the leading edge. This vertically down flow induced by the static pressure field of the inner duct exit flow is likely to generate measurable additional thrust force for the DDF based vehicle.

Exemplary Embodiments of Double Ducted Fan geometries: The standard or conventional duct and three possible variations of the Double Ducted Fan (DDF) concept described in this study are presented in Figures F, and G, H, and I. Three dimensional solid models of the four duct configurations, a horizontal cross section and a vertical cross section are included in these figures.

CASE-A as shown in Figure G is termed as the Tall DDF. The Tall DDF is able to generate a higher thrust in hover position than that of "only" the standard duct containing an identical rotor. However, in forward flight, due to the extended axial chord of the outer duct, the nose-up pitching moment generation can be present in this duct design. This design has a throat section located at the trailing edge of the duct airfoils. Since the axial chord of the outer duct is longer than that of the inner duct this design may have a slight drag penalty when compared to the standard ducted fan.

Figure H shows the most effective Double Ducted Fan (DDF) configuration **CASE-B** since it has the ability to generate an amount of thrust when compared to that of the "only" standard ducted fan configuration. Another important characteristic of CASE-B is its ability to operate without enhancing the nose-up pitching moment of the vehicle in forward flight. This configuration was analyzed in great detail mainly because of its combined ability to enhance thrust and reduce nose-up pitching moment in forward flight without a substantial drag increase.

An **ECCENTRIC DOUBLE DUCTED FAN** (DDF) concept is also shown in Figure I. This concept requires a movable outer duct in order to control the throat area in the intermediate duct of the vehicle for a highly optimized forward flight performance. Variable throat mechanism introduced in this concept provides a greater range of operation in a DDF type vehicle offering a more accurate lip flow control over a much wider forward flight velocity range. Figure H shows a highly blocked second duct that

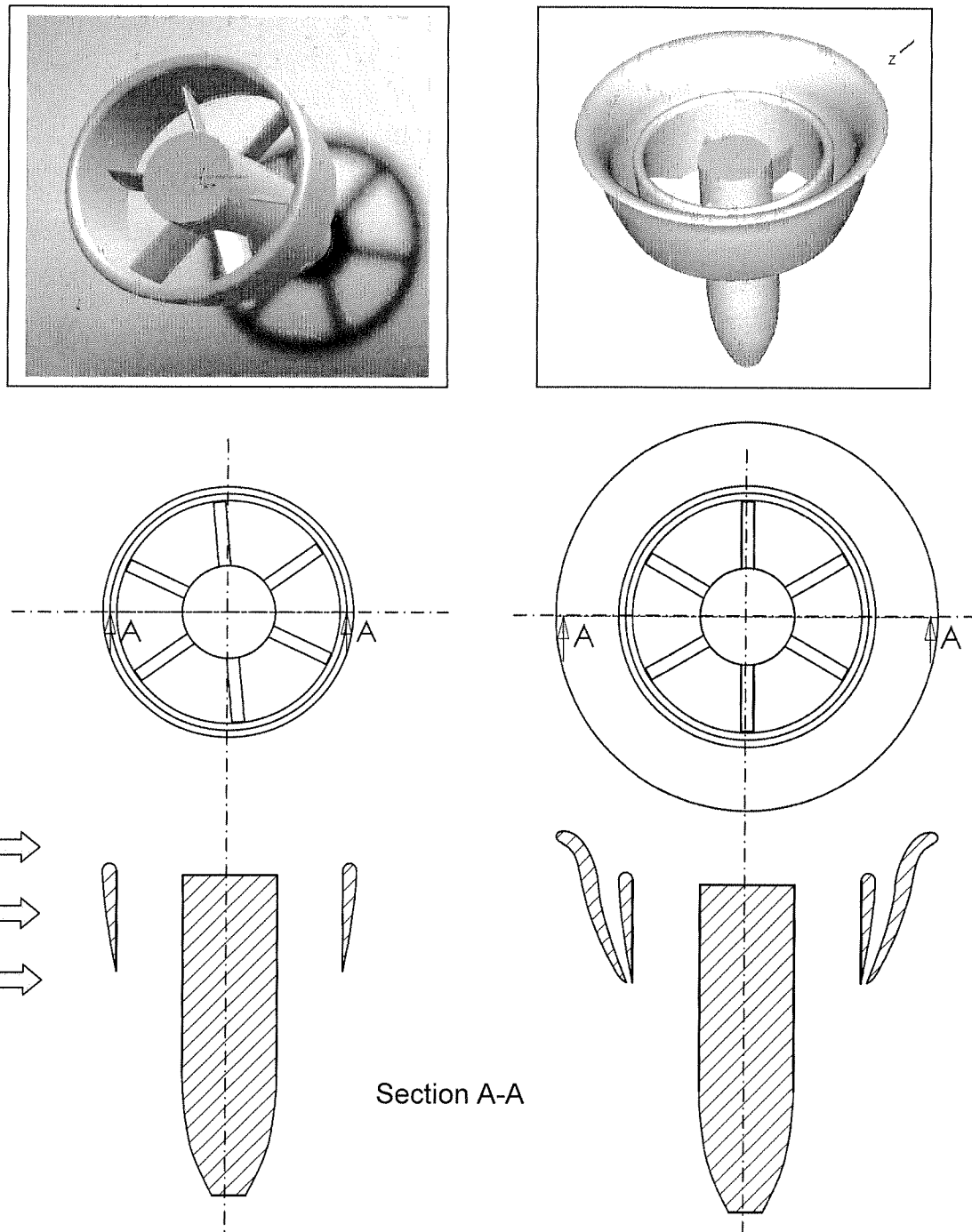


**Figure F. Baseline ducted fan
(Standard duct)**

**Figure G. CASE-A
Tall Double Ducted Fan (DDF)**

is proper for very low forward flight velocity. It is required that the throat area is enlarged by moving the outer duct as the forward flight velocity is increased. Although an almost optimal lip separation control can be achieved with an eccentric (DDF), its mechanical complexity and weight penalty is obvious. The outer duct airfoil definition of this concept is the same as CASE-B that is described in detail in Figure E(b).

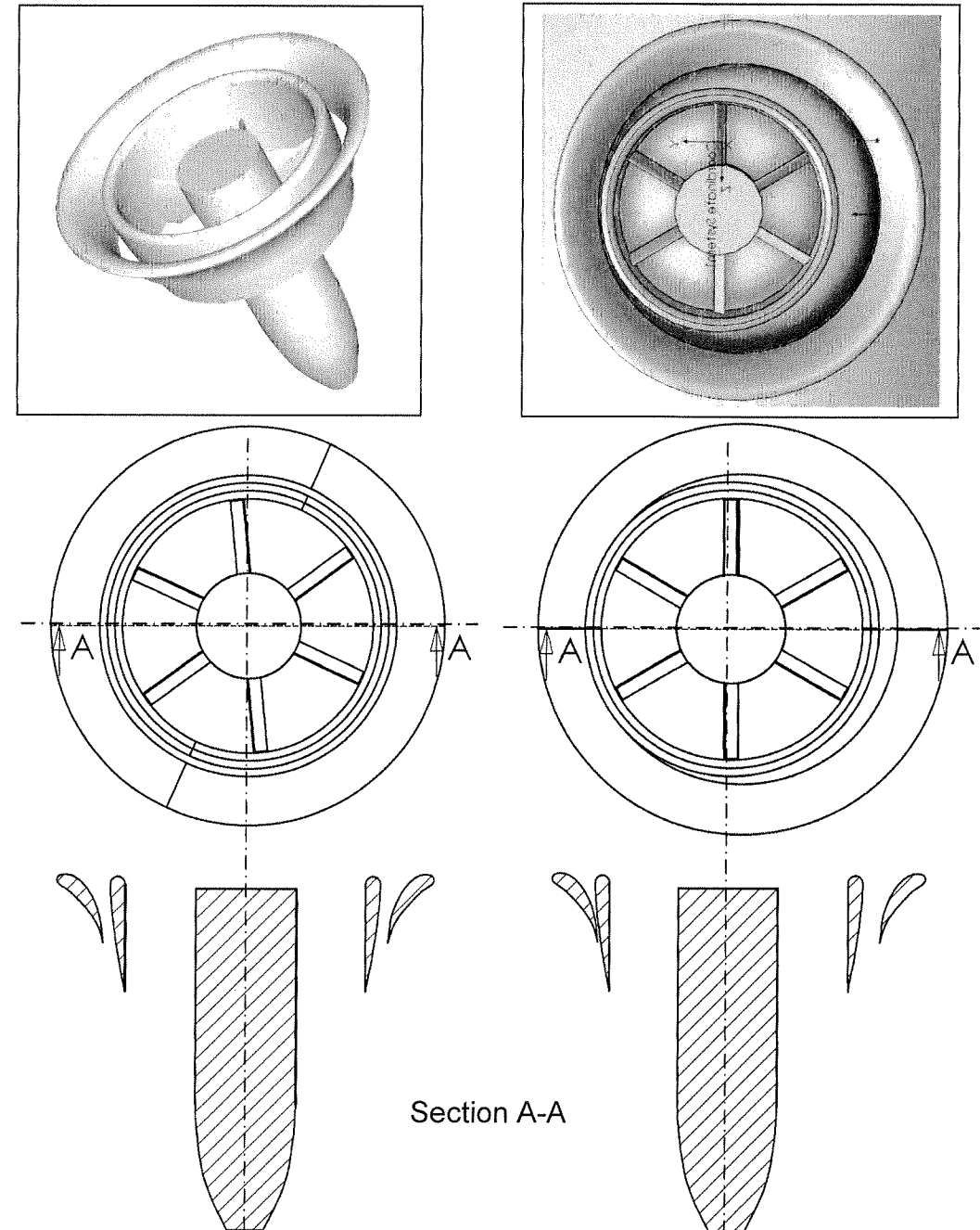


Figure H. CASE-B
Short Double Ducted Fan (DDF)

Figure I.
Eccentric Short Double Ducted Fan (DDF)

APPENDIX

B

METHOD OF ANALYSIS USED IN (DDF) CONCEPT DEVELOPMENT:

A three dimensional simulation of the mean flow field around the ducted fan was performed using a custom developed actuator disk model implemented into the commercial code Ansys/Fluent. The specific computational system solves the Reynolds Averaged Navier-Stokes (RANS) equations using a finite volume method. The transport equations describing the flow field are solved in the specific domain that is discretized by using an unstructured computational mesh. For the analysis of the 3D viscous flow field around ducted fan rotors there are a few potential computational models. The most complex and time consuming computational model is the modeling of unsteady, viscous, and turbulent flow in and around the fan rotor by using a 3D precision model of the rotor geometry using a sliding mesh technique. This type of solution is usually lengthy and requires significant computer resources especially in the forward flight mode when an axisymmetric flow assumption is not applicable. The current RANS computations use a simplified rotor model termed as "actuator disk model" for the simulation of the general flow features of the fan rotor. A $k-\epsilon$ turbulence model was invoked for the current computations for all parts of the computational domain remaining outside the rotor disk area.

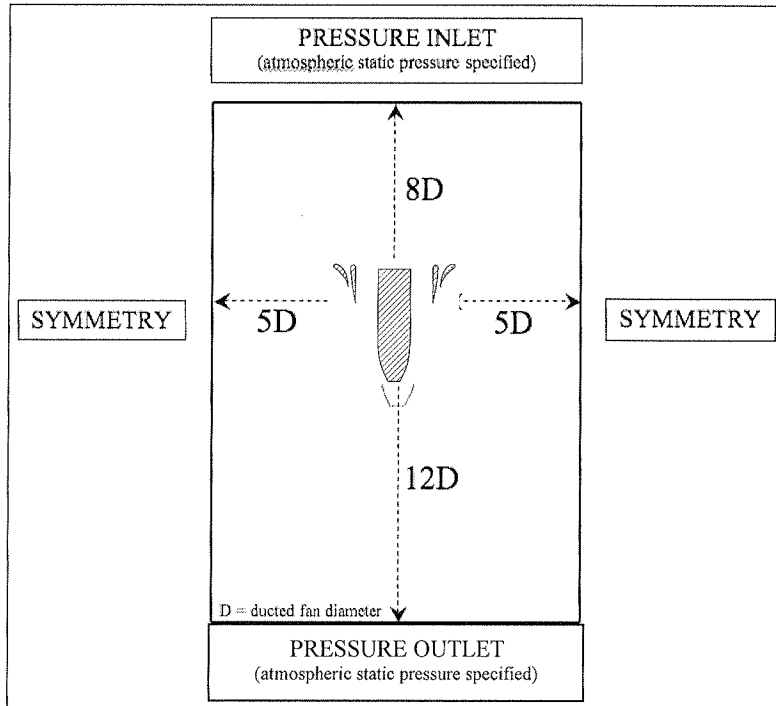


Figure J. The computational domain and the boundary conditions for RANS simulations (drawing not to scale)

Boundary conditions: Three dimensional and incompressible Navier-Stokes equations are solved in the computational domain since the tip Mach number of the current fan is about $M=0.28$. Figure D shows the specific boundary conditions implemented in the

solver. The duct and the tail-cone surfaces are considered as solid walls with no-slip condition. On the side surfaces of the domain, a symmetry condition is assumed. For the hover condition, a pressure inlet boundary is assumed on the top surface where atmospheric static pressure is prescribed. Pressure inlet boundary is treated as loss-free transition from stagnation to inlet conditions. The solver calculates the static pressure and velocity at the inlet. Mass flux through the boundary varies depending on interior solution and specified flow direction. Pressure outlet boundary condition is assumed on the bottom surface for hovering condition. Pressure outlet boundary interpreted as atmospheric static pressure of the environment into which the flow exhausts. An additional "Fan" type condition was set using a "simplified rotor model" replacing the ducted fan rotor.

A simplified rotor model: A highly time efficient simplification of flow modeling across the rotor is implemented in this study. The complex 3D rotor flow field in the rotating frame of reference is replaced by a simplified and custom designed "actuator disk model" derived from the simultaneous use of the energy equation, radial equilibrium equation, and the conservation of angular momentum principle across the fan rotor. The radial equilibrium equation is the inviscid force balance in radial direction at a given spanwise position, balancing the pressure forces in with the centrifugal force. The viscous effects are ignored in this simplified and easy to implement "actuator disk model".

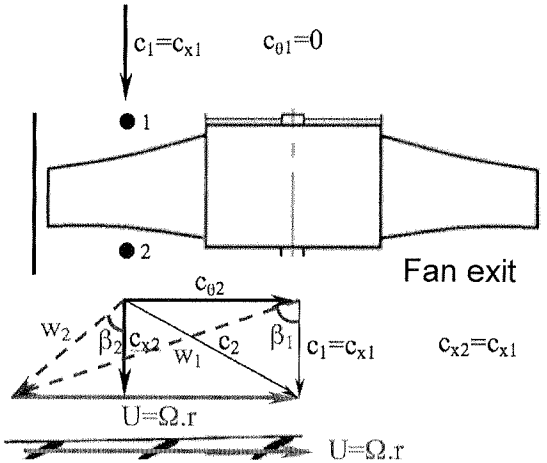


Figure K. Velocity triangles at the inlet and exit of the ducted fan rotor

In the present simplified rotor model, a static pressure change term between points 1 and 2 is computed at each radial position of the rotor from hub to tip, Figure K. The magnitude of the static pressure jump term across the rotor is closely related to the amount of stagnation enthalpy change from the rotor inlet to exit. The stagnation enthalpy increase from the rotor inlet to exit is the same as the rate of energy provided to the fluid by the rotor per unit mass flow rate of the duct flow. The conservation of

angular momentum principle and energy equation suggests that the magnitude of this jump is mainly controlled by the tangential (swirl) component of the flow velocity $c_{\theta 2}$ in the absolute frame of reference at the exit of the rotor and rotor angular speed Ω .

Velocity triangles: Figure K presents the velocity triangles of the ducted fan rotor at inlet (1) and exit (2). β_1 and β_2 are the blade inlet and exit angles measured from the axial direction. Since the maximum possible tip Mach number (0.28) of the rotor is not in the compressible flow range, it is reasonable to assume that the internal energy at the rotor inlet e_1 and exit e_2 is the same, $e_1=e_2$. In a ducted fan rotor, it is realistic to assume that the "axial component" of the absolute velocity vector is also conserved from inlet to exit $c_{x2}=c_{x1}$. The flow is assumed to be axial at rotor inlet where $c_1=c_{x1}$ and there is now swirl at rotor inlet, $c_{\theta 1}=0$. The relative velocity vector at the exit of the rotor w_2 is smaller than the relative velocity w_1 at the rotor inlet. While the relative flow w_2 is diffusing in the relative frame of reference, the absolute flow velocity vector c_2 is accelerated at the rotor exit, because of added energy to the flow by the rotor.

Pressure jump across the rotor: Equation (1) represents the change of stagnation enthalpy in the ducted fan rotor system. The right hand side of this equation is the rate of work per unit mass flow rate of air passing through the rotor. The right hand side is also the same as the product of the rotor torque and angular speed of the fan rotor. The right hand side can be computed by considering the conservation of angular momentum between rotor inlet and exit at a selected rotor angular speed Ω .

$$(h_{\text{st}2} - h_{\text{st}1}) = U(c_{\theta 2} - c_{\theta 1}) \quad \text{where } U = \Omega r \text{ and } c_{\theta 1} = 0 \quad (1)$$

$$[(h_i + c_i^2/2) - (h_i + c_i^2/2)] = Uc_{\theta 2} \quad (2)$$

$$[(e_2 + \frac{p_2}{\rho_2} + c_2^2/2) - (e_1 + \frac{p_1}{\rho_1} + c_1^2/2)] = Uc_{\theta 2} \quad (3)$$

Equation (1) is a simplified form of the energy equation from rotor inlet to exit of a ducted fan unit. When $e_1=e_2$ is substituted into equation (3) because of incompressibility condition, the "Euler equation" or "pump equation" results in, as shown in equation (4). Using equations (4) and (5), an final equation for the calculation of static pressure jump between the rotor inlet and exit can be obtained for the specific rotor design used in the current study.

Calculating the rotor exit swirl velocity $c_{\theta 2}$: The determination of $c_{\theta 2}$ is performed by using the velocity triangles that are shown in Figure E. The blade inlet/exit angle distribution for β_1 and β_2 in radial direction is known from the existing rotor geometrical properties as shown in Table 1. w_2 is calculated from the assumption $c_{x2}=c_{x1}=c_1$. The absolute rotor exit velocity c_2 is determined by vectorially adding $U=\Omega r$ to w_2 .

$$\frac{1}{\rho} (P_{\theta 2} - P_{\theta 1}) = U c_{\theta 2}$$

$$\frac{1}{\rho} \left[\left(p_2 + \rho \frac{c_2^2}{2} \right) - \left(p_1 + \rho \frac{c_1^2}{2} \right) \right] = U c_{\theta 2} \quad (5)$$

$$\Delta p = p_2 - p_1 = \rho \left[U c_{\theta 2} - \frac{1}{2} (c_2^2 - c_1^2) \right] \quad (6)$$

Equation (6) allows prescribing a pressure jump Δp in function of radial position, rotor angular speed Ω , density, rotor exit swirl velocity $c_{\theta 2}$, c_1 and c_2 . The rate of energy (per unit mass flow rate) added to the flow by the rotor is specified by the product $U.c_{\theta 2}$ as shown in equations (4) and (5). Equation (6) could be evaluated at each radial position between the rotor hub and tip resulting in the radial distribution of the static pressure jump required by the general purpose viscous flow solver for a "Fan" type boundary condition. Δp can be effectively specified in a user defined function "UDF" in the solver. The "Fan" type boundary condition is an effective and time efficient method of implementing a rotor flow field via an "actuator disk model" in a 3D viscous flow computation.

Air breathing character of (DDF) in forward flight: Table 1 presents the computed fan rotor mass flow rate for all ducted fan types studied in this paper for both hover and forward flight conditions. In addition to hover conditions, the results are also presented

	Fan Mass Flow rate (kg/s)	Thrust (N)	Pitching Moment (N.m)	Flight Condition
Baseline Duct	0.301	3.04	0.00	No Crosswind (Hover)
Baseline Duct	0.291	3.47	0.17	10 m/s Crosswind
Baseline Duct	0.201	3.11	0.27	20 m/s Crosswind
MODIFIED DUCTS (DDF)				
Case A	0.313	4.93	0.37	10 m/s Crosswind
Case A	0.261	5.07	0.83	20 m/s Crosswind
Case B	0.295	3.72	0.16	10 m/s Crosswind
Case B	0.280	4.86	0.29	20 m/s Crosswind

Table 1. Computed rotor mass flow rate for all fan configurations during hover and forward flight

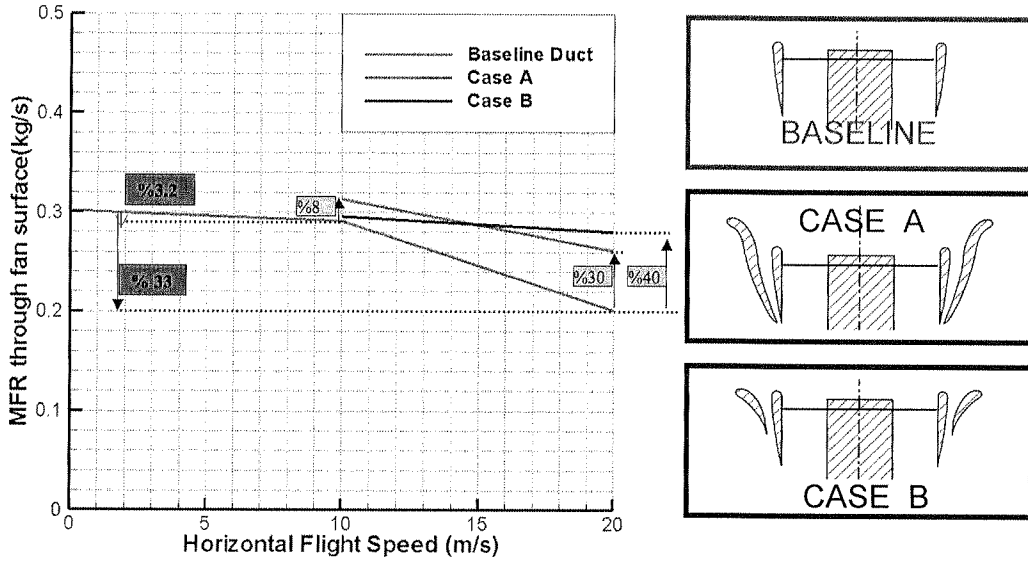


Figure L. Rotor disk mass flow rate versus forward flight speed at 9000 rpm

for 10 m/s and 20 m/s forward flight velocities at 9000 rpm rotor speed that is constant for all computations. Constant rpm flow simulations provide a basis for comparisons of 3D mean flow, fan thrust, nose-up pitching moment, total pressure and static pressure fields. Although the rotor speed is constant for all computations, the amount of mechanical energy transferred to the air during its passage through the rotor varies, because of highly varying inlet flow field into the ducted fan unit during hover, forward flight at 10 m/s and 20 m/s. Table 1 also provides the computational estimates of thrust, nose-up pitching moment for hover and forward flight conditions.

Figure L shows that the baseline duct suffers from a high level of “inlet flow distortion” at 10 m/s and 20 m/s forward flight velocity. The overall mass flow rate passing from the ducted fan is reduced to 66 % of the hover mass flow rate as shown by the red line in Figure L (for 20 m/s forward flight). This limitation on the rotor mass flow rate is mainly the result of the large separated flow region occurring at just downstream of the lip section of the leading side of the duct. While the leading side of the baseline duct passes a severely limited amount of air mass, the trailing side of the duct is able to breathe at a better rate than the leading side. It is apparent that the leading side of the baseline duct is partially blocked at high forward flight velocities. Figure L also shows a drop in rotor mass flow rate when the forward flight velocity is increased from 10 m/s to 20 m/s.

Baseline duct mass flow rate, thrust and nose-up pitching moment: Table 1 contains nose-up pitching moment information for all flight regimes showing a measurable increase in the pitching moment when the baseline vehicle moves at 10 m/s and 20 m/s in comparison to hover conditions. The nose-up pitching moment is measured with respect to the center of gravity of the ducted fan unit for all cases. At 20 m/s forward flight condition, the predicted pitching moment is 1.6 times that of the pitching moment

at 10 m/s flight velocity. The pitching moment generation on a typical ducted fan in forward flight is directly related to the extent of inlet lip separation, the impingement of the rotor inlet flow on the duct inner surface (aft casing surface) on the trailing side of the duct, imbalance of the rotor exit field between the leading side (low momentum) and trailing side (high momentum), aerodynamic profiling of the duct outer surface especially near the leading side.

Predicted baseline ducted fan thrust values at 10 m/s and 20 m/s increase to 1.5 times and 1.7 times of the thrust of the baseline duct at hover conditions. This relative thrust enhancement is due to the specific external shape of the baseline duct and modified rotor inlet conditions at elevated forward speed levels.

Mass flow rate, thrust and nose-up pitching moment characteristics of CASE-A : The air breathing character of the baseline duct can be enhanced by implementing the tall double ducted fan (DDF) designated as CASE-A as shown in Figure L. The mass flow rate of CASE-A is about 8 % more than that of the baseline duct operating at the forward speed of 10 m/s. The rotor mass flow rate enhancement for CASE-A at 20 m/s is much higher than that of the baseline duct operating at 20 m/s. A 30 % enhancement over the baseline duct is possible. This relative mass flow rate enhancement is a direct result of reduced inlet lip separation near the leading side of the duct designs at forward flight.

The predicted thrust for the tall double ducted fan (DDF) CASE-A is markedly higher than that of the baseline duct. At 10 m/s horizontal flight velocity, the thrust of CASE-A is about 1.7 times that of the baseline duct. When the flight velocity is elevated to 20 m/s, CASE-B produces an augmented thrust value of 1.9 times that of the baseline duct. The reduction of the inlet lip separation results in a direct enhancement of the ducted fan exit flow near the leading side of the duct. The thrust enhancements are due to both ducted fan exit flow enhancements near the leading side of the unit, the external aerodynamic shape of the outer duct. The leading side of the DDF CASE-A rotor plane breathes air from the inlet at a much-enhanced rate than that of the trailing side. The tall (DDF) CASE-A also entrains a measurable amount of air into the outer duct from the inlet area of the unit especially near the trailing side. The flow in the outer duct is in opposite direction to the rotor flow near the leading side. However, the outer duct flow for the circumferential positions away from the leading side of the duct is in the same direction as the main rotor flow direction. Additional thrust augmentation is possible in the outer duct at positions away from the leading edge.

Although the tall (DDF) CASE-A is an excellent thrust producer at high forward flight velocities, it has the capability of augmenting the usually unwanted nose-up pitching moment mainly because of the external shape of the outer lip at elevated forward flight velocities. The pitching moment predicted at 10 m/s is about 2.2 times that of the baseline duct. At 20 m/s, the pitching moment produced by CASE-A is about 3.1 times

that of the baseline duct value. The reason the short ducted fan CASE-B was designed and developed was the need to reduce the unwanted pitching up moment generation unique to CASE-A.

An effective DDF design CASE-B with highly reduced nose-up pitching moment: CASE-B as shown in Figure L is a shorter version of the double ducted fan design concept. CASE-B is designed to produce a reduced nose-up pitching moment when compared to CASE-A. Another goal with CASE-B is to obtain similar thrust gains over the baseline duct. The short double ducted fan (DDF) CASE-B controls the lip separation as effectively as the tall (DDF) CASE-A without producing a high nose-up pitching moment. The airfoil geometry forming the outer duct has an axial chord length that is about half of the axial chord of the inner duct (also termed as standard fan or baseline fan). A detailed description of obtaining a short double ducted fan (DDF) CASE-B is given in Figure E starting from a baseline duct. Figure 9 indicates that the mass flow rate enhancement (black line) of CASE-B is very similar to CASE-A (blue line). The short (DDF) CASE-B's sensitivity to increasing forward flight velocity is much less when compared to tall (DDF) CASE-A. Implementation of a second duct as shown in Figure 6.b enhances the lip separation controlled flight zone further into higher forward flight velocities. The thrust values predicted for the short (DDF) are much higher than the standard duct predictions at 10 m/s and 20 m/s. There is a slight reduction in thrust when comparison is made against the tall (DDF) CASE-A. CASE-B has the ability to control nose-up pitching moment effectively. The pitching moment generation for the short (DDF) CASE-B is very much suppressed when compared to tall (DDF) CASE-A. CASE-B nose-up pitching moments are about the same as the values predicted for the baseline duct. The short (DDF) concept described in Figure 6.b is a highly effective scheme of improving the lip separation related inlet flow distortion problem for the rotor of a ducted fan based VTOL/STOL vehicle. CASE-B is able to enhance thrust without increasing the nose-up pitching moment generation. Since the leading side of the fan exit jet is well balanced against the trailing side of the exit jet, the effectiveness of the control surfaces at the exit of the ducted fan are expected to function much effectively for the short (DDF) CASE-B.

Rotor inlet total pressure deficit at elevated forward flight speed for the baseline ducted fan: Figure M shows the total pressure obtained just upstream of the baseline ducted fan rotor for hover, and two forward flight velocities. The spanwise total pressure distribution (red symbols) between the duct leading edge and trailing edge for hover condition shows a relatively flat total pressure distribution at the inlet surface. The inlet field is symmetrical between the leading side and trailing side along a radial line passing from the axis of rotation.

When the baseline ducted fan increases its forward flight speed to 10 m/s, a very visible inlet total pressure defect due to leading side lip separation is apparent as shown by the green symbols in Figure M. At 20 m/s forward flight speed, the total pressure defect

near the leading side of the duct can be increased (blue symbols). The low momentum fluid entering the leading side of the rotor occupies a much wider portion of the blade span.

The trailing side of the rotor shows a very different inlet total pressure distribution along the flight direction as shown in Figure M. The inlet flow passing over the inlet plane tends to stagnate on the trailing side of the baseline duct aft surface (casing) due to the specific orientation of inlet streamlines in this region, especially at elevated forward flight velocities. The green and blue symbols representing 10 m/s and 20 m/s forward flight velocities show the elevated levels of total pressure near the trailing side of the duct inner surface. This type of total pressure augmentation only occurring during forward flight is directly related to an unwanted drag force acting in opposite direction to forward flight direction.

Figure M also reveals another local flow separation zone in the trailing side of the baseline duct inlet surface. The inlet flow progressing to enter into the trailing portion of the duct also separates from the corner of the rotor hub surface, generating a low momentum zone as shown in Figure M.

Figure M clearly shows the imbalance between the leading side and trailing side of the duct inlet flow field in terms of local total pressure. The duct has tremendous difficulty in terms of air breathing action near the leading side of the duct. Due to blocked nature of the leading side flow, the trailing side sees an inlet flow with an unnecessarily elevated level of total pressure near the casing surface. However there is a total pressure deficit near the hub surface for forward flight conditions due to rotor hub corner separation.

Rotor inlet flow distortion reduction character of (DDF) CASE-B: The short double ducted fan (DDF) CASE-B has an ability to control the inlet lip separation leading to enhanced thrust and well controlled nose-up pitching moment. Figure N shows the lip separation enhancements of CASE-B in comparison to the baseline duct. The red square symbols define the rotor inlet total pressure distribution in spanwise direction for the baseline fan under hover conditions. The inlet flow under hover conditions may not have inlet flow distortion for the baseline ducted fan.

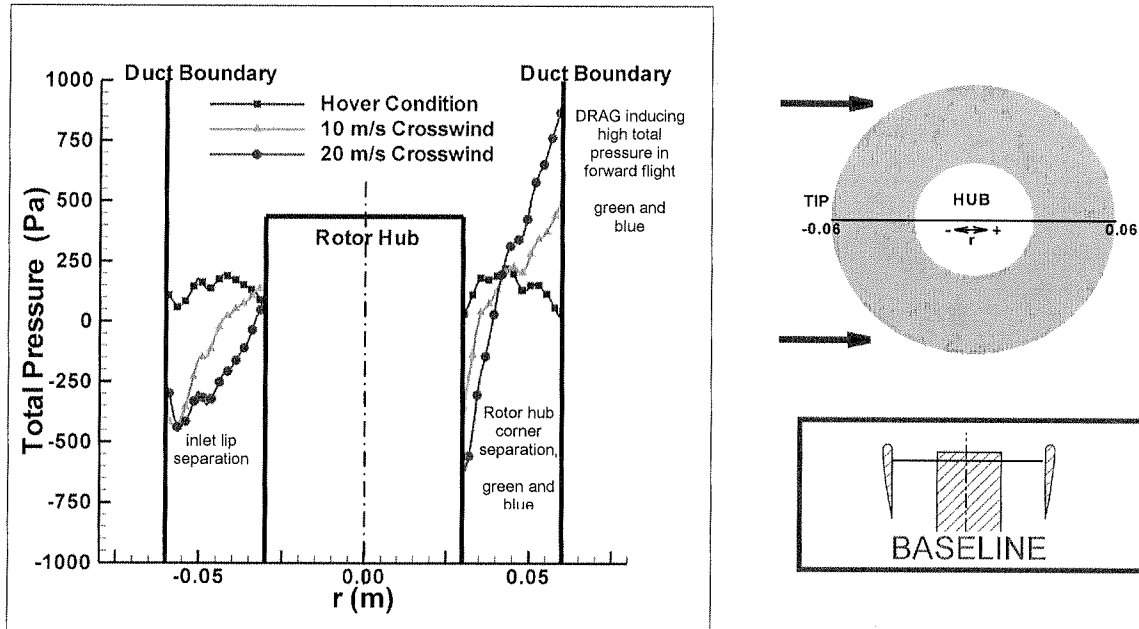


Figure M. Rotor inlet total pressure deficit at elevated forward flight speed for the baseline ducted fan

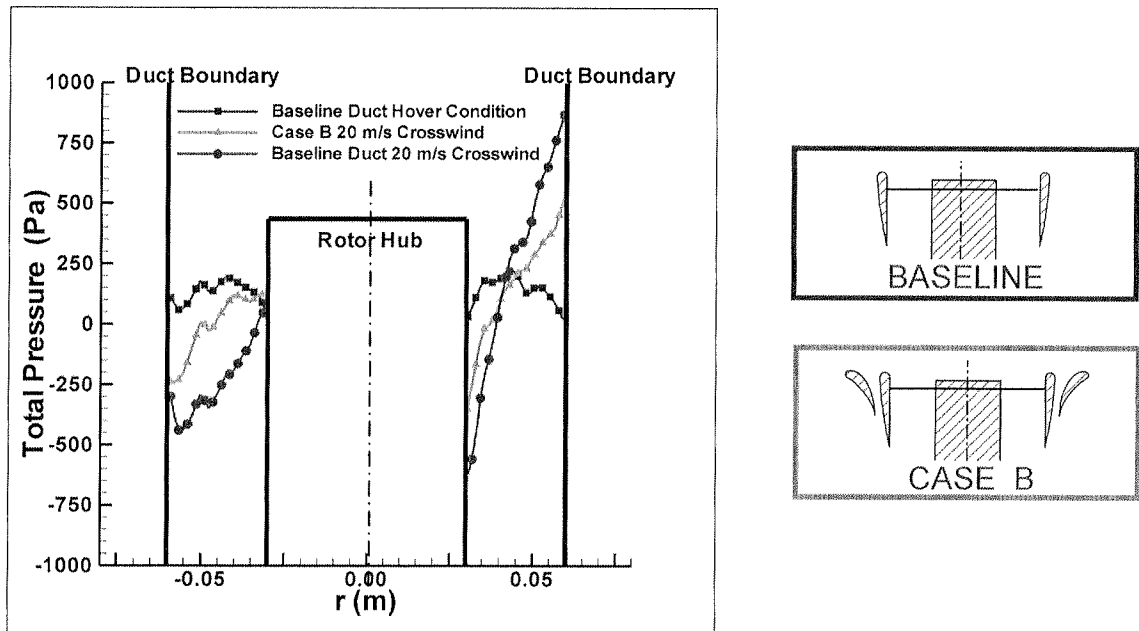


Figure N. Reduction in rotor inlet flow distortion between the leading side and trailing side of (DDF) CASE-B short double ducted fan

Inlet flow character of the baseline ducted fan in horizontal flight is represented by the blue circular symbols for the forward flight speed of 20 m/s. The green triangular symbol shows the inlet total pressure distribution generated by the short double ducted fan (DDF) CASE-B. The inlet lip separation related total pressure deficit of the baseline configuration is effectively reduced by the use of the short double-ducted fan (DDF) CASE-B (green triangular symbols in Figure M). The local mass flow rate passing from the leading side of the duct is much enhanced because of the short double-ducted fan (DDF) CASE-B. The unnecessarily elevated total pressure observed near the aft casing of the baseline ducted fan (trailing side) as shown by blue circular symbols is also controlled when CASE-B is implemented (green triangular symbols). This reduction of total pressure on the trailing side of (DDF) CASE-B is beneficial in balancing the leading side and trailing side flow of the fan rotor exit flow field. CASE-B also reduces drag generation occurring near the aft part of the casing.

A comparative evaluation of local velocity magnitude, streamlines and total pressure for all three ducts: As part of the (DDF) concept validation, local flow field details including magnitude of velocity, streamlines and total pressure distributions are presented over a surface passing through the duct leading edge, axis of rotation and the trailing edge of the duct system. Comparisons of the specific (DDF) design against the corresponding baseline duct at 9000 rpm are discussed using the computational predictions explained in the previous paragraphs.

CASE-A tall (DDF) versus baseline duct results at 10 m/s and 20 m/s: Figure O compares the flow fields of tall double ducted fan designated as CASE-A and the baseline duct. A slight forward lip separation is observed at 10 m/s forward flight velocity. The tall double ducted fan CASE-A produces an enhanced thrust level of 1.73 times that of the baseline ducted fan at 10 m/s. The mass flow rate of CASE-A at 9000 rpm is also enhanced when compared to the baseline ducted fan, as shown in Figure 12. The total pressure distributions clearly show the low momentum regions due to inlet lip separation and hub corner separation on the rotor disk inlet surface as shown by dark blue areas in Figure O. The tall ducted fan provides a reduction in the size of the low momentum flow areas downstream of the inlet lip and hub corner when compared to the baseline duct.

Although the “hub corner separation” area is relatively smaller than the “inlet lip separation” area, the flow blockage created by the hub corner separation affects the flow downstream of the rotor as shown in Figure O. A total pressure imbalance can be observed at downstream of the rotor for the baseline duct. The existence of the tall double ducted fan CASE-A slightly enhances the total pressure on the leading side of the rotor exit flow for 10 m/s forward flight velocity.

Figure O explains the nature of inlet flow distortion existing in the baseline duct and tall double ducted fan design at 10 m/s forward flight velocity by using local total pressure predictions. The dark blue zone near the leading side of the baseline ducted fan shows the highest level of aerodynamic loss resulting from “**inlet lip separation**” at 10 m/s. This area is where the relative flow tends to separate because of the existence of the duct lip near the leading side. The fan inlet surface also has another aerodynamic loss region at just downstream of the “**hub corner**” on the trailing side of the duct. The

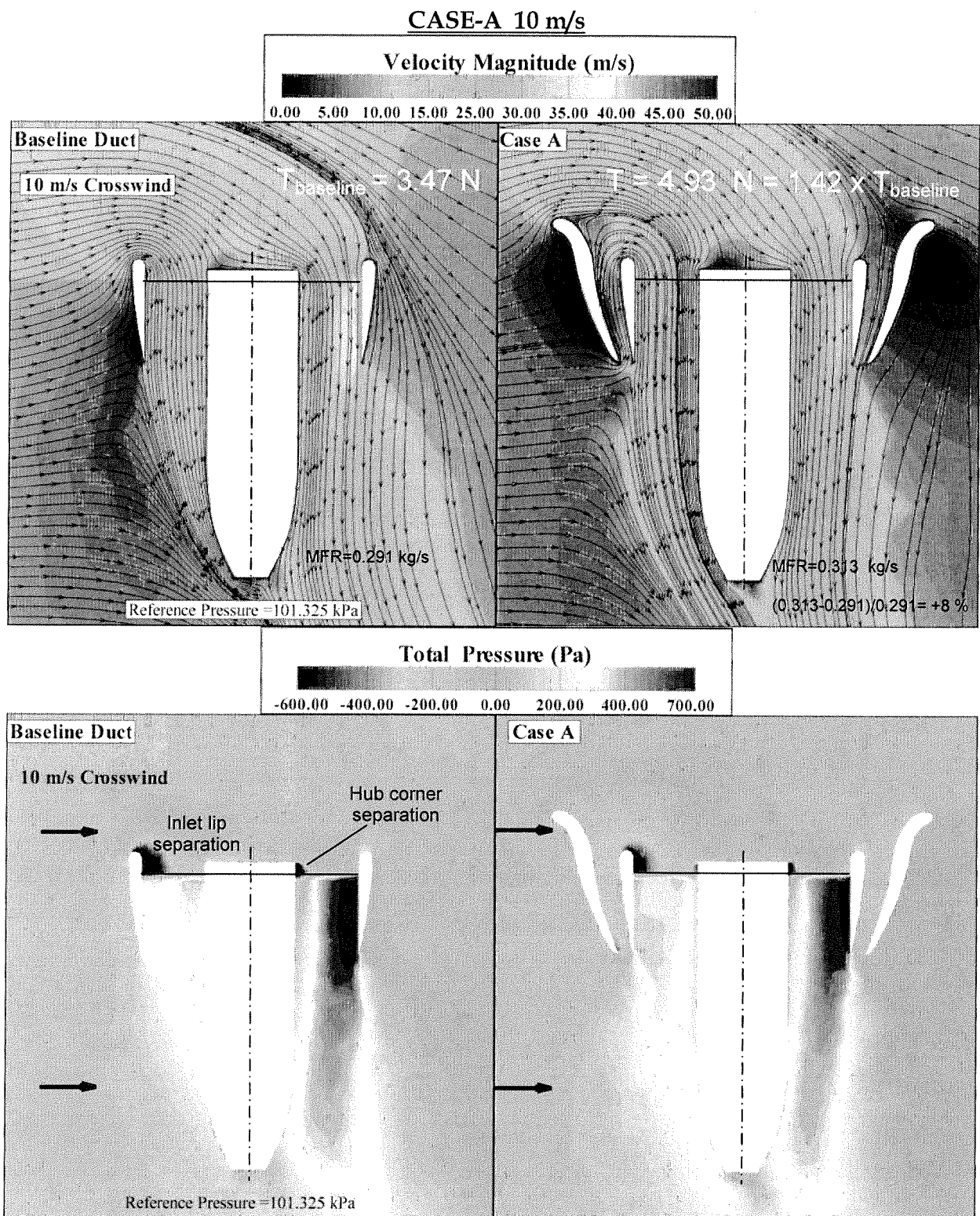


Figure O. Velocity Magnitude and total pressure distribution, baseline duct versus CASE-A tall double ducted fan (DDF) at 10 m/s forward flight velocity

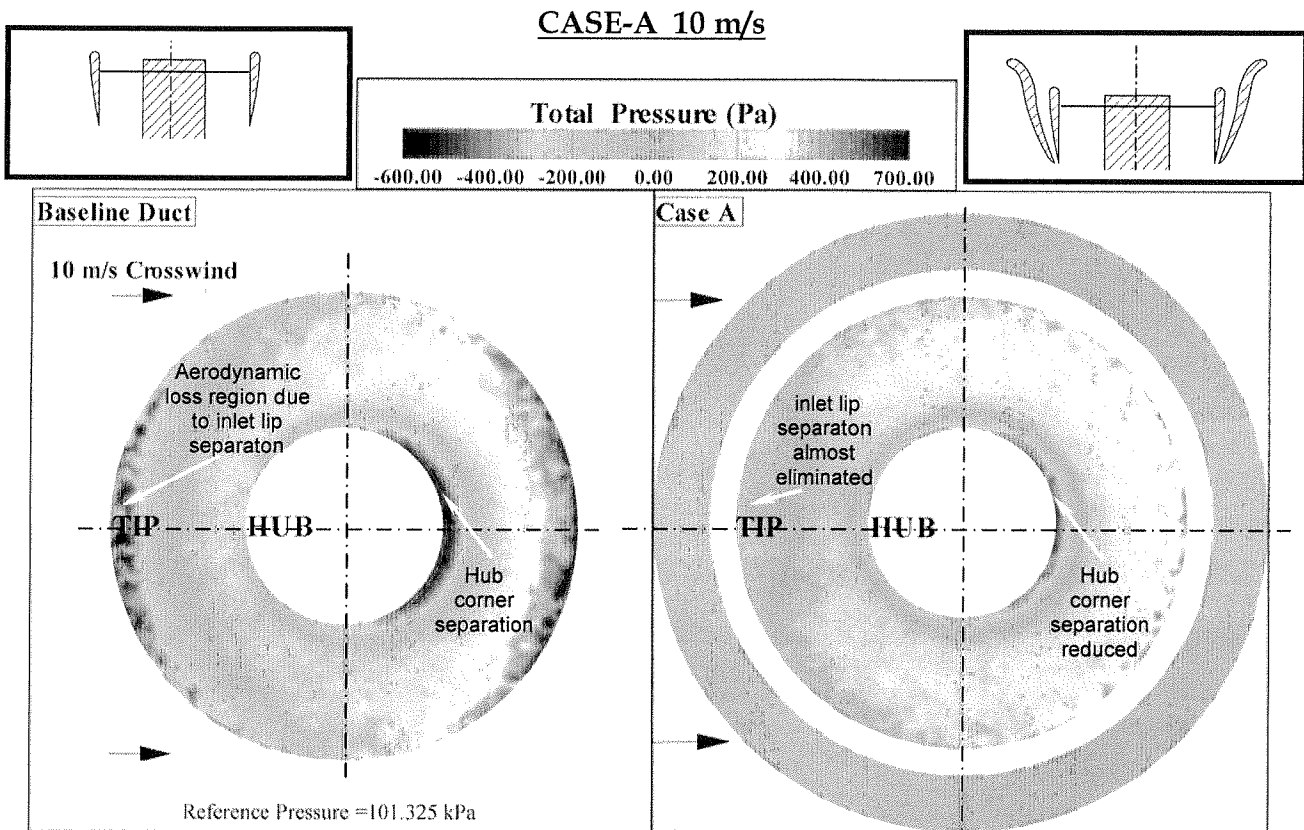


Figure P. Total pressure distribution at rotor inlet plane (horizontal) baseline duct versus CASE-A tall double ducted fan (DDF) at 10 m/s forward flight velocity

beneficial influence of the tall double ducted fan design CASE-A is shown in Figure P. The aerodynamic loss areas indicated by the dark blue zones in the baseline duct distribution are effectively reduced in the tall double ducted fan design. The red total pressure zone near the trailing side of the baseline duct shows the highest levels of total pressure over the inlet plane. This excessive level of total pressure is the result of the inlet lip separation induced inlet flow distortion when the leading side of the duct loses its ability to breath effectively. The trailing side tends to pass most of the inlet mass flow rate including the fluid that is skipping over (deflected by) the lip separation region. This is a common observation in most standard ducted fans in horizontal flight. The aft part of the fan usually generates additional drag force because of this red high total pressure zone at the inlet plane. The implementation of the tall double ducted fan makes the total pressure distortion near the trailing side of the duct less significant. The red zone with the highest total pressure for the baseline duct is almost eliminated for the double ducted fan design CASE-A. The inlet flow distortion is efficiently dealt with the implementation of the second duct configuration termed as CASE-A, Figure P.

When forward flight velocity is increased to 20 m/s, Figure Q shows the highly adverse character of the separated flow zone behind the inlet lip section in the baseline duct. The flow also tends to separate behind the hub corner on the trailing side of the duct. Figure Q demonstrates that the flow is nearly blocked by the existence of a large separated flow zone and the flow is effectively induced into the trailing side of the duct. The imbalance in the local mass flow rate between the leading side of the duct and the trailing side of the duct at 20 m/s is much more apparent when compared to 10 m/s results. Figure Q displays the flow enhancement in the lip separation area for the tall double ducted fan (DDF) CASE-A. The re-circulatory flow is almost eliminated downstream of the lip. The leading side of the duct starts breathing effectively because of CASE-A's ability to eliminate inlet flow distortion near the leading side. The (DDF) CASE-A results show a low momentum region that could be viewed as a three dimensional wake region behind the vehicle at 20 m/s forward flight velocity. The outer duct flow near the leading side is in a direction opposite to rotor flow direction. The outer duct flow near the leading side is an essential component of the (DDF) concept because of its highly important role in reversing the inner lip region separated flow conditions. The outer duct flow smoothly reverses into the rotor flow direction away from the leading side.

The inlet plane total pressure distribution shown in Figure R, (DDF) CASE-A reveals a reduction in lip separation leading to a substantially uniform inlet flow distribution between the leading side and trailing side of the inner duct. The DDF duct local flow distribution at the rotor exit is much enhanced in comparison to the baseline duct. Hub corner separation area is also reduced in (DDF) CASE-A. Most circumferential positions of the second duct (other than the leading side of the duct) contributes to the generation of thrust because of the measurable outer duct flow observed in this area

CASE-B short (DDF) versus baseline duct results at 10 m/s and 20 m/s: Figures S and T show the most effective double ducted fan (DDF) treatment results obtained for a forward flight velocity of 10 m/s. A detailed geometrical definition of the short double ducted fan (DDF) CASE-B was discussed in Figure 6.b. The short DDF has the ability to enhance thrust in relative to the baseline case without producing a nose-up pitching moment by effectively reducing inlet lip separation and hub corner separation areas. The short double ducted fan configuration is a self adjusting lip separation control system preserving its separation control features in a wide range of forward flight velocities. The effectiveness of the short DDF treatment is shown in the total pressure distribution presented in Figure S for 10 m/s flight velocity. In addition to the area reduction of the separated flow areas (dark blue), the total pressure imbalance between the leading side and trailing side is eliminated. The leading side of the inner duct of the short DDF CASE-B breathes at a much enhanced rate when compared to the baseline case. The red high total pressure areas provide a well-balanced fan exit jet near the leading side and trailing side of the fan.

Figure T indicates a high level of inlet total pressure uniformity for CASE-B in contrast to the strong inlet flow distortion generated by the baseline duct. When short double ducted fan is used, the lip separation and hub corner separation control is highly effective at 10 m/s flight velocity. The red high total pressure zone occurring near the trailing side of the baseline duct inlet is also converted into a lower total pressure field. This reduction is effective in reducing the high drag production apparent in the baseline duct.

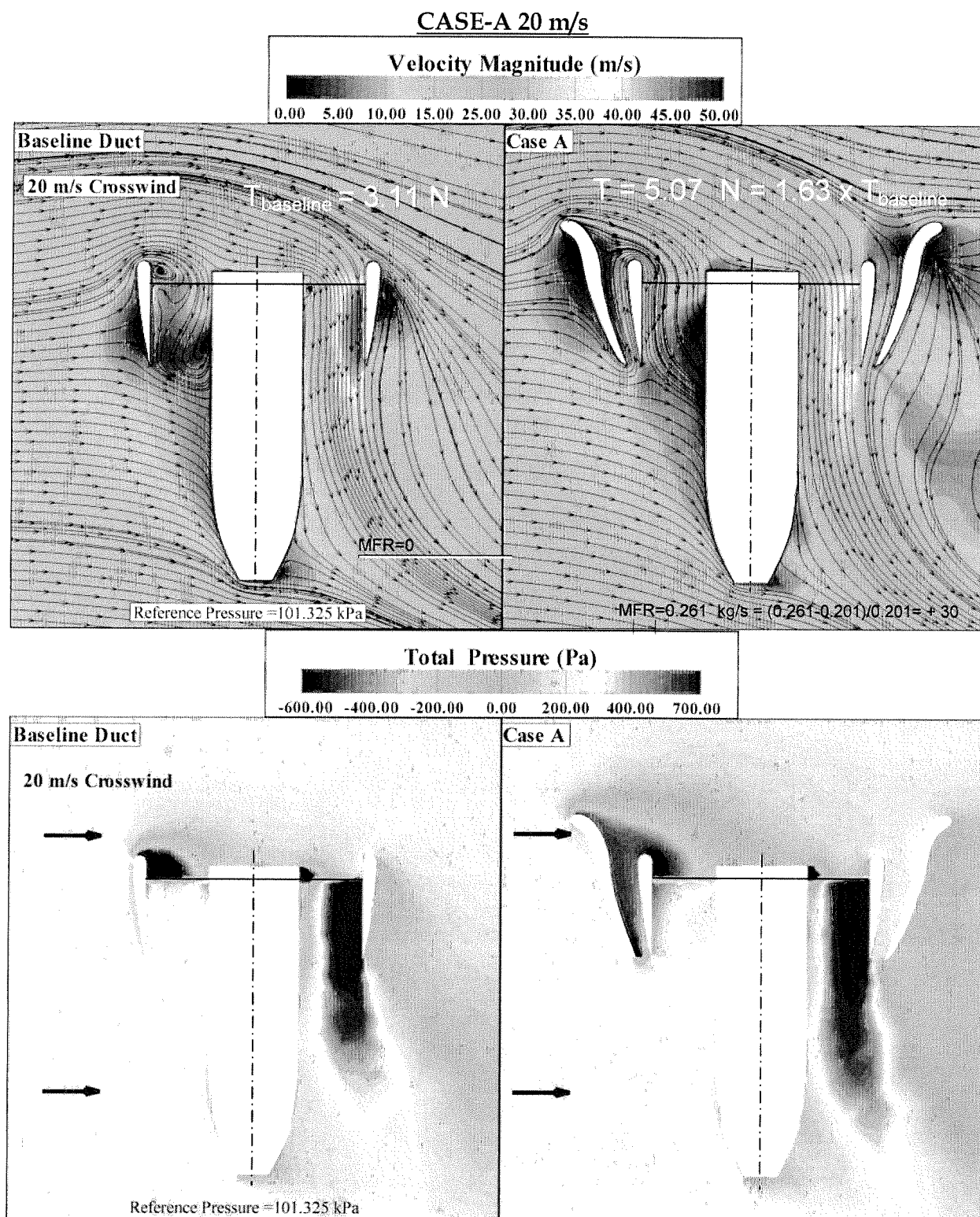


Figure Q. Velocity Magnitude and total pressure distribution, baseline duct versus CASE-A tall double ducted fan (DDF) at 20 m/s forward flight velocity

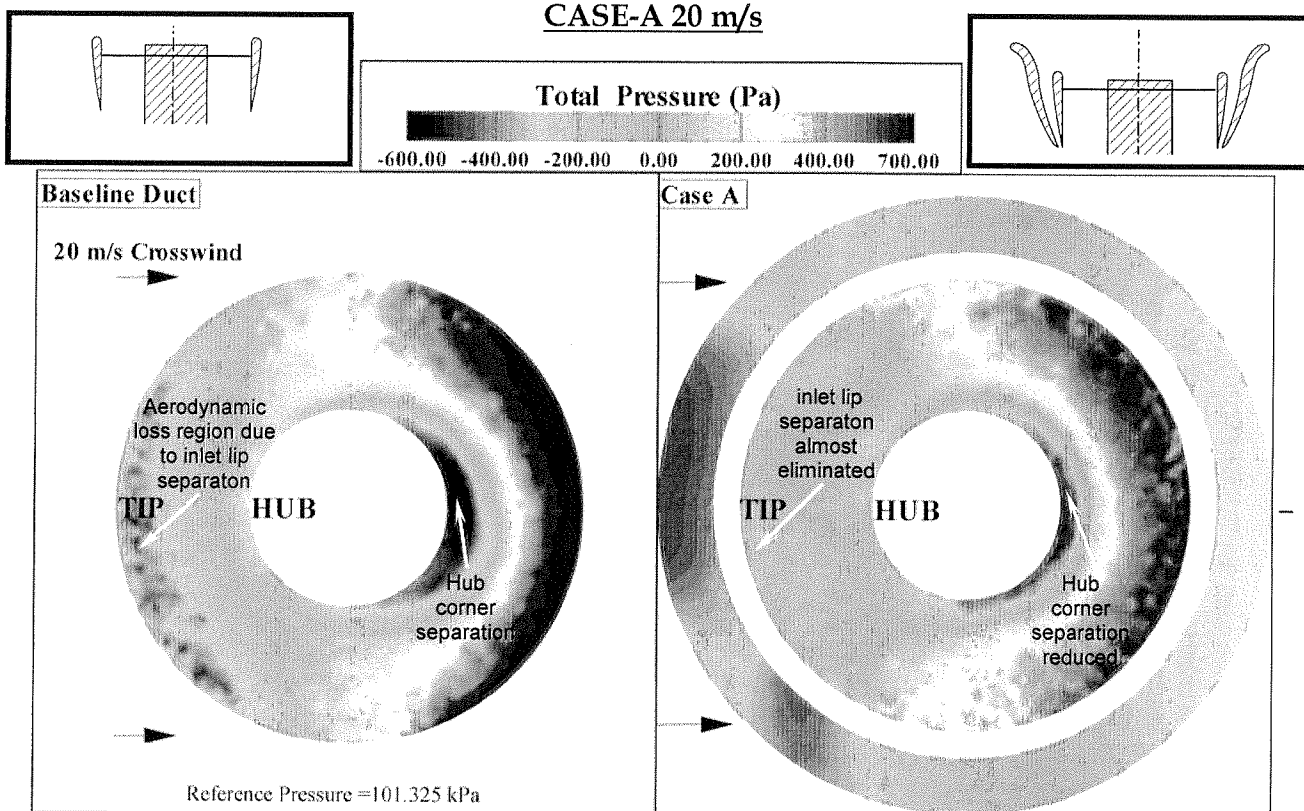


Figure R. Total pressure distribution at rotor inlet plane (horizontal) baseline duct versus CASE-A tall double ducted fan (DDF) at 20 m/s forward flight velocity

When the short double ducted fan arrangement (DDF) CASE-B is evaluated at 20 m/s flight velocity, the loss elimination features near the leading side lip, hub corner area are apparent. Highly separated lip region flow adversely blocking the leading side of the inner duct is successfully dealt with the flow control features of the short (DDF) as shown in Figure U. A well-balanced short (DDF) exit flow provides a higher level of thrust when compared to the baseline duct. The flow enhancements and thrust enhancement from the short (DDF) comes with no additional nose-up pitching moment generation as explained in Table 1. and Figure U. A highly effective inlet flow distortion control ability of the short ducted fan is apparent in Figure V. A vehicle using the short (DDF) concept CASE-B generates a higher level of thrust with a well balanced ducted fan exit flow without excessive generation of nose-up pitching moment. This approach results in enhancements of the performance of the control surfaces and enhanced range because the energy efficiency of the ducted fan is enhanced. The elimination of severe inlet flow distortion is likely to enhance the rotor exit flow quality before further interaction with typical control surfaces.

CASE-B 10 m/s

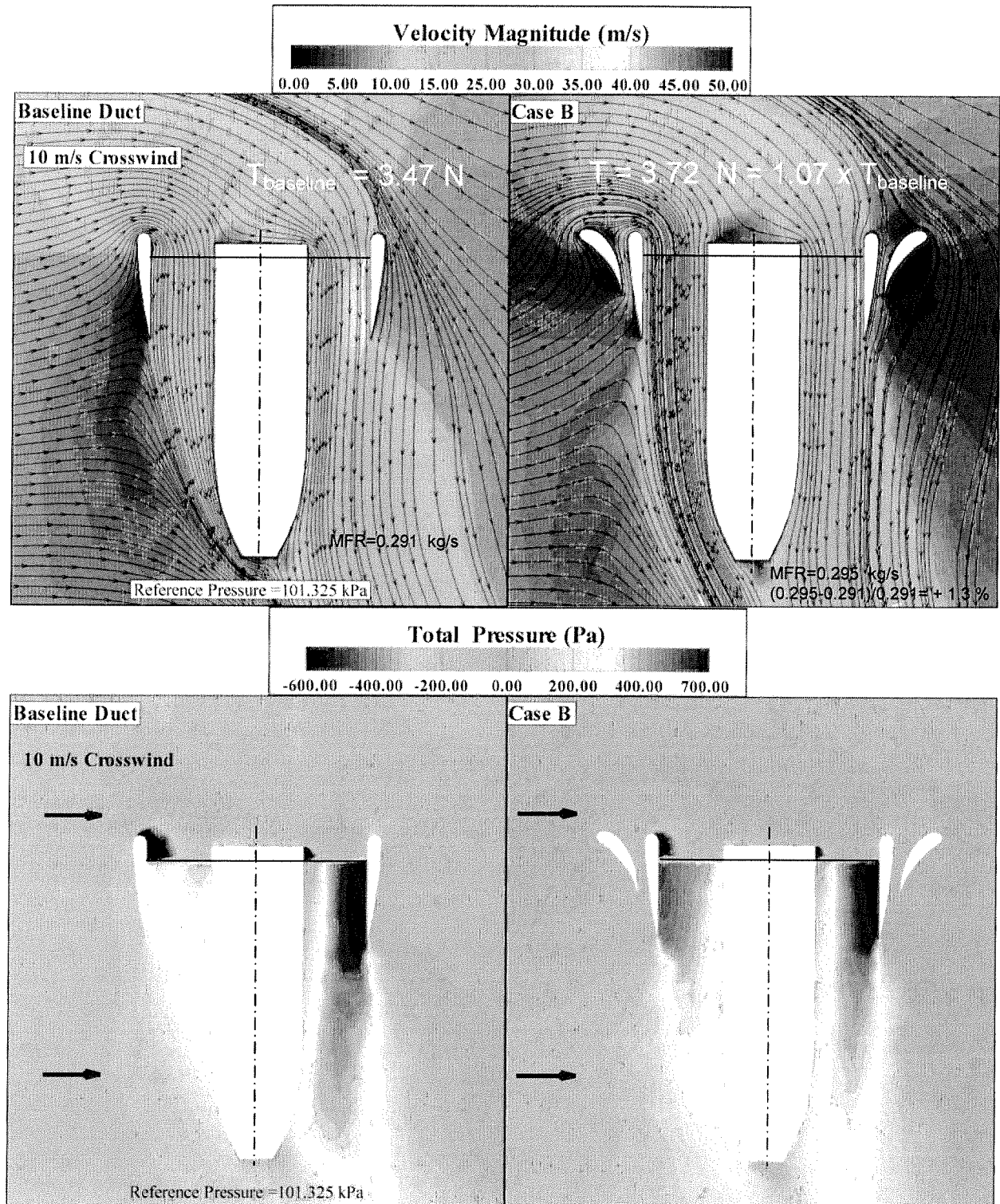


Figure S. Velocity Magnitude and total pressure distribution, baseline duct versus CASE-B short double ducted fan (DDF) at 10 m/s forward flight velocity

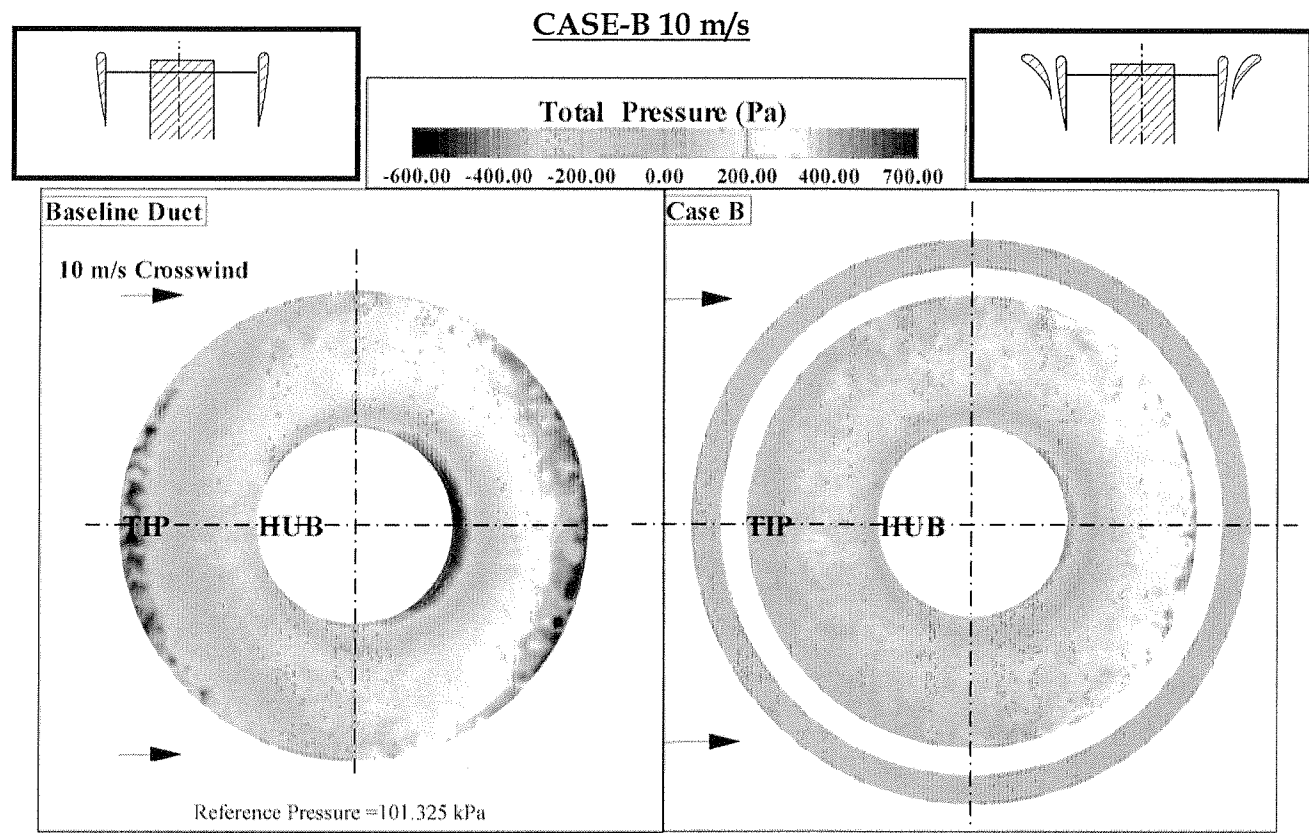


Figure T. Total pressure distribution at rotor inlet plane (horizontal)
baseline duct versus CASE-B short double ducted fan (DDF)
at 10 m/s forward flight velocity

CASE-B 20 m/s

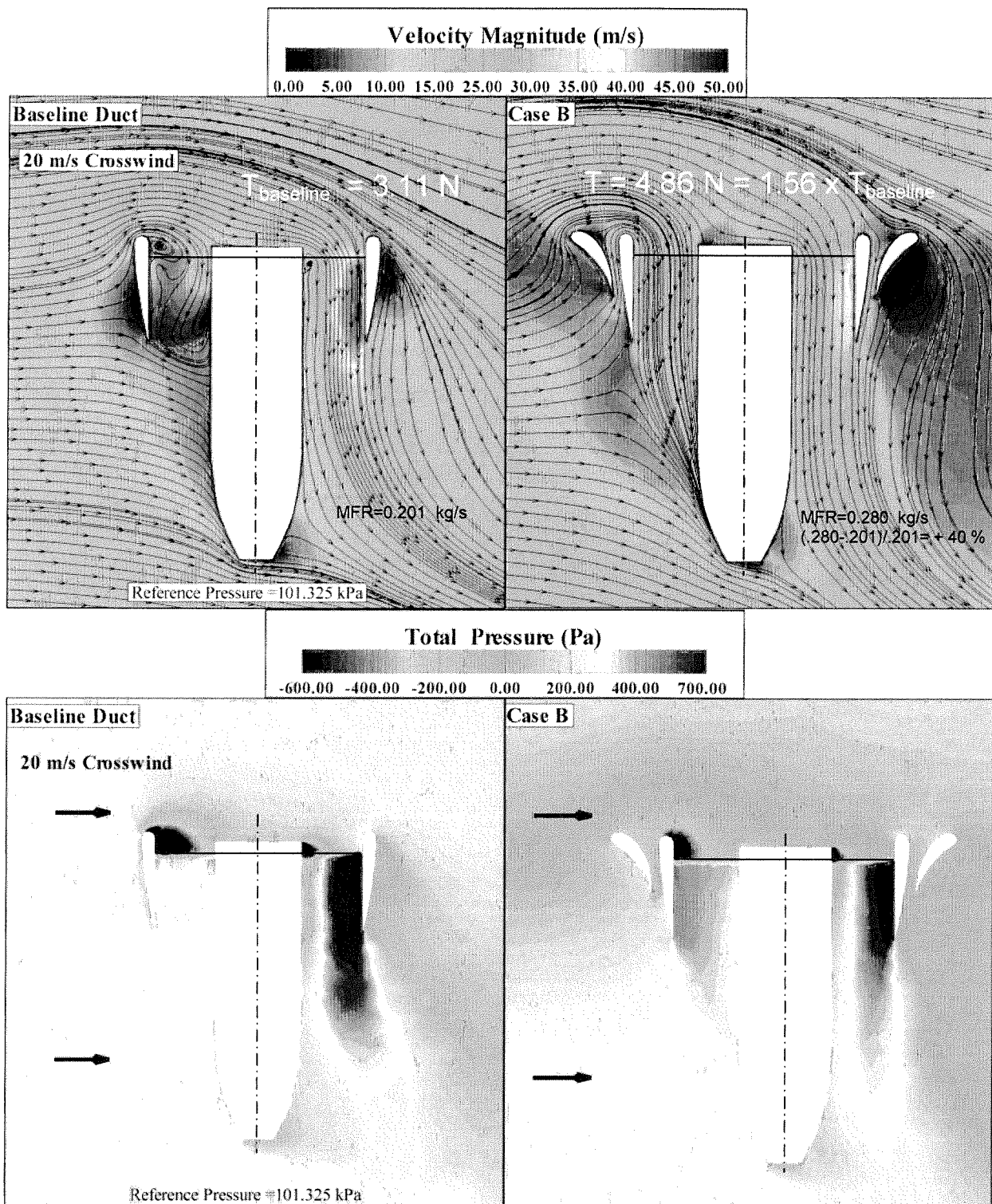


Figure U. Velocity Magnitude and total pressure distribution,
baseline duct versus CASE-B short double ducted fan (DDF)
at 20 m/s forward flight velocity

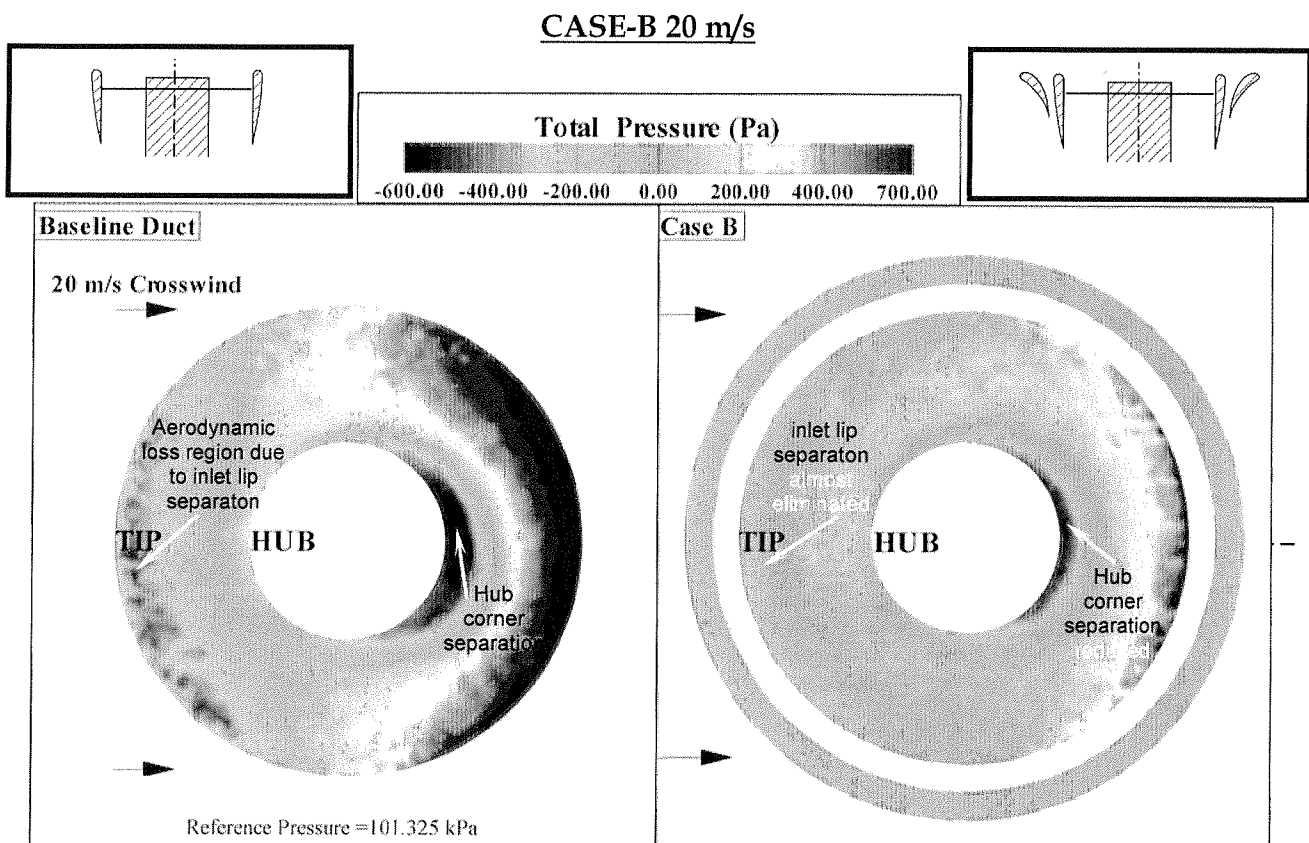


Figure V. Total pressure distribution at rotor inlet plane (horizontal) baseline duct versus CASE-B short double ducted fan (DDF) at 20 m/s forward flight velocity

Upstream lip region local flow enhancements in (DDF): Figure W defines the local sampling locations for static pressure and skin friction coefficient on the airfoil of the inner duct at the leading edge location. The lowercase characters represent the “rotor side” locations and the uppercase characters show the “outer side” sampling locations for static pressure and skin friction coefficient on the inner duct airfoil section.

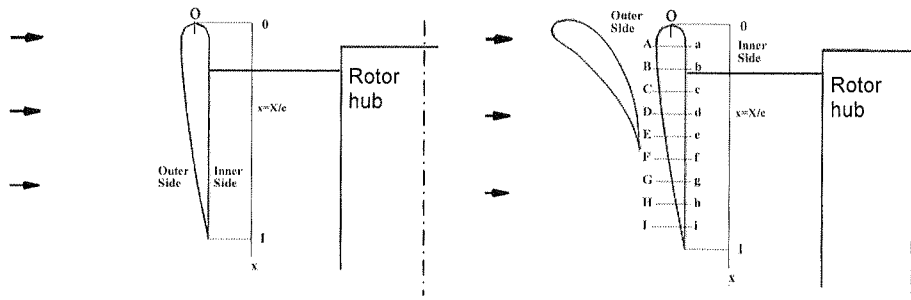


Figure W.

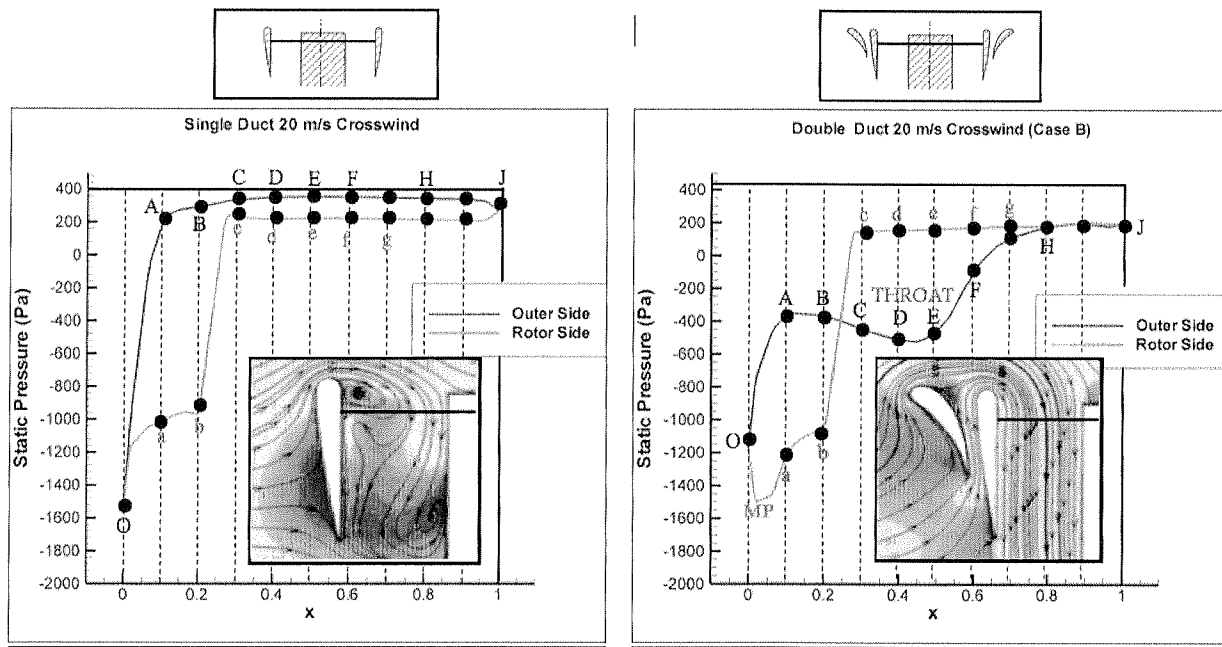


Figure X. Comparison of the static pressure distribution on the baseline lip section and inner duct lip section of the (DDF) CASE-B airfoil

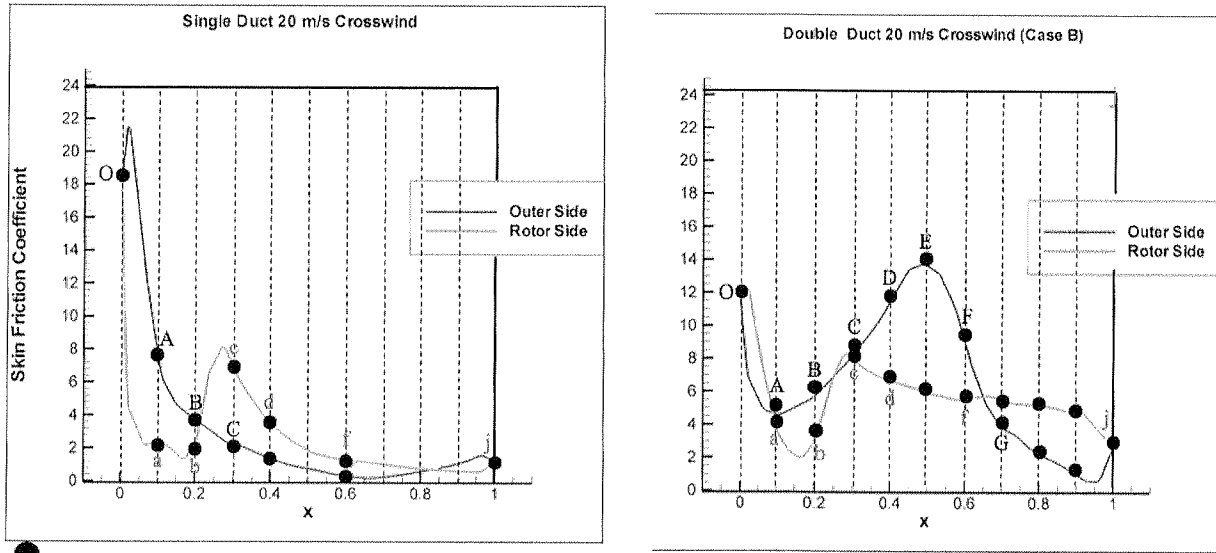


Figure Y. Comparison of the skin friction coefficient distribution on the baseline lip section and inner duct lip section of the (DDF) airfoil

Static pressure distribution around the lip section of the baseline duct: Figure X shows the static pressure distribution for the baseline duct and double ducted fan (DDF) CASE-B for the forward flight velocity of 20 m/s. The distributions presented in Figure X are plotted at the leading edge of the duct. The pressure gradient occurring around the leading edge radius of the inner duct can control the leading edge lip separation problem. The external flow stagnates on the leading side of the baseline duct at point D as shown in Figure X. Figure U shows the stagnation area (dark blue color). The approaching flow to the duct is divided into a stream reaching up to the leading edge and a second stream approaching down to the trailing edge of the duct airfoil. The static (or stagnation) pressure from point D to J remains constant. The external flow slightly accelerates to the leading edge point from point C to A for the baseline duct. There is a tremendous acceleration zone between point A and the leading edge point O, as clearly shown by the favorable pressure gradient between the point A and O. This is the area within the leading edge diameter of the lip section. The geometrical leading edge point O is the minimum pressure point for the baseline duct airfoil. The flow on the inner side of the lip sees a very strong adverse pressure gradient around the leading edge circle. The strong flow separation character shown in Figures X and U is mainly due to the strong adverse pressure gradient affecting the boundary layer growth between points O, a and finally b. The rotor process described in equations from 1 to 6 results in the sudden pressure rise on the inner part of the baseline duct between b and c.

Static pressure distribution around the lip section of the double ducted fan (DDF): Figure X also shows the static pressure distribution around the lip section of the short double ducted fan (DDF) CASE-B. The external static pressure distribution in the outer duct section is established by the external flow in forward flight. The (DDF) outer duct flow that is proceeding vertically up generates a unique wall static pressure distribution in a converging diverging channel. The external flow in horizontal flight stagnates on the shorter outer airfoil and turns towards the leading edge of the outer duct airfoil. Most of the flow stagnating at the lower part of the vehicle is directed towards the converging diverging channel of the outer duct. There is a stagnation region between points J and H on the outer side of the inner duct. The flow accelerates towards the throat section of the outer duct. The throat section is usually between points E and D. The flow after the throat section smoothly decelerates up to point A that is very close to the leading edge circle of the leading edge. The existence of the diverging channel is responsible from a much softer acceleration around the leading edge diameter of the lip section between A and O. The flow is still accelerating when it is passing through the geometrical leading edge point O. The minimum pressure point in (DDF) configuration is on the inner side of the lip section at $x=X/c=0.03$. The flow starts decelerating after this minimum pressure point MP. The adverse pressure gradient region after the minimum pressure point MP in (DDF) is much shorter and the adverse pressure gradient between MP and a is much milder than that of the baseline duct. Figure X clearly shows the modified nature of the static pressure distribution around the lip section of (DDF) leading to the elimination of the severe inlet lip separation region that is unique to the baseline duct in forward flight. The (DDF) approach is extremely useful in controlling the adverse pressure gradient region (or the separated flow content) occurring on the inside surface of the lip region.

Skin friction distribution around the leading edge of the duct: Figure Y presents the skin friction coefficient distributions on the baseline duct lip section and inner duct lip section of the (DDF) configuration. The lowest level of predicted wall shear stress is on the lip surface along the separated flow region for the baseline duct. This low momentum region is between points O and a corresponding to the highest level of adverse pressure gradients before the rotor inlet plane. The overall level of wall shear stress is higher between points a and b for the double duct configuration showing the immediate influence of weakened adverse pressure gradients resulting from the (DDF) geometry.

The double ducted fan inlet flow conditioning concept that can substantially enhance the performance and controllability of V/STOL "vertical/short take-off and landing" vehicles, UAVs "uninhabited aerial vehicles" and many other ducted fan based systems. The DDF concept developed in this study addresses the technical problems in ducted fans operating at almost 90 ° angle of attack, in the forward flight mode. The technical problems related to this mode of operation are as follows:

- ⇒ Increased aerodynamic losses and temporal instability of the fan rotor flow when "inlet flow distortion" from "the lip separation area" finds its way into the tip clearance gap leading to the loss of energy addition capability of the rotor.
- ⇒ Reduced thrust generation from the upstream side of the duct due to the rotor breathing low-momentum re-circulatory turbulent flow.
- ⇒ A severe imbalance of the duct inner static pressure field resulting from low momentum fluid entering into the rotor on the leading side and high momentum fluid unnecessarily energized on the trailing side of the rotor.
- ⇒ A measurable increase in power demand and fuel consumption when the lip separation occurs to keep up with a given operational task.
- ⇒ Lip separation and its interaction with the tip gap flow requires a much more complex vehicle control system because of the severe non-uniformity of the exit jet in circumferential direction and excessive pitch-up moment generation.
- ⇒ At low horizontal speeds a severe limitation in the rate of descent and vehicle controllability may occur because of more pronounced lip separation. Low power requirement of a typical descent results in a lower disk loading and more pronounced lip separation.
- ⇒ Excessive noise and vibration from the rotor working with an inlet flow distortion.
- ⇒ Very complex unsteady interactions of duct exit flow with control surfaces.

The double ducted fan uses a secondary stationary duct system to control "inlet lip separation" related momentum deficit at the inlet of the fan rotor occurring at elevated forward flight velocities. The DDF is self-adjusting in a wide forward flight velocity regime. DDFs corrective aerodynamic influence becomes more pronounced with increasing flight velocity due to its inherent design properties. The DDF can also be implemented as a "Variable Double Ducted Fan" (VDDF) for a much more effective inlet lip separation control in a wide range of horizontal flight velocities in UAVs, air vehicles, trains, buses, marine vehicles and any axial flow fan system where there is lip separation distorting the inlet flow. Most axial flow fans are designed for an inlet flow with zero or minimal inlet flow distortion. The DDF concept is proven to be an effective way of dealing with inlet flow distortions occurring near the tip section of any axial flow fan rotor system operating at high angle of attack.

CLAIMS

1. A ducted air rotor comprising:

a hub;

a rotor fan having a plurality of blades rotatably coupled to the hub, said plurality of blades having an inlet side and an outlet side;

a first duct and a second duct, wherein the first duct circumscribes the rotor fan and the second duct circumscribes at least a portion of the first duct; and

a channel defined between the first duct and the second duct.

2. The ducted air rotor of claim 1, wherein the second duct is movable relative to the first duct to adjust at least a portion of the channel.

3. The ducted air rotor of claim 1, wherein said channel configured to direct air flow cross-wise to the first duct over a top of the first duct into the inlet side of the fan.

4. The ducted air rotor of claim 1, wherein the second duct is oriented axially upward from a leading edge of the first duct such that an axial distance is between the leading edge of the first duct and a leading edge of the second duct.

5. The ducted air rotor of claim 1, wherein the second duct is oriented at an angle with respect to the first duct.

6. The ducted air rotor of claim 1, wherein the second duct is cambered.

7. The ducted air rotor of claim 1, wherein the second duct has an airfoil shape.

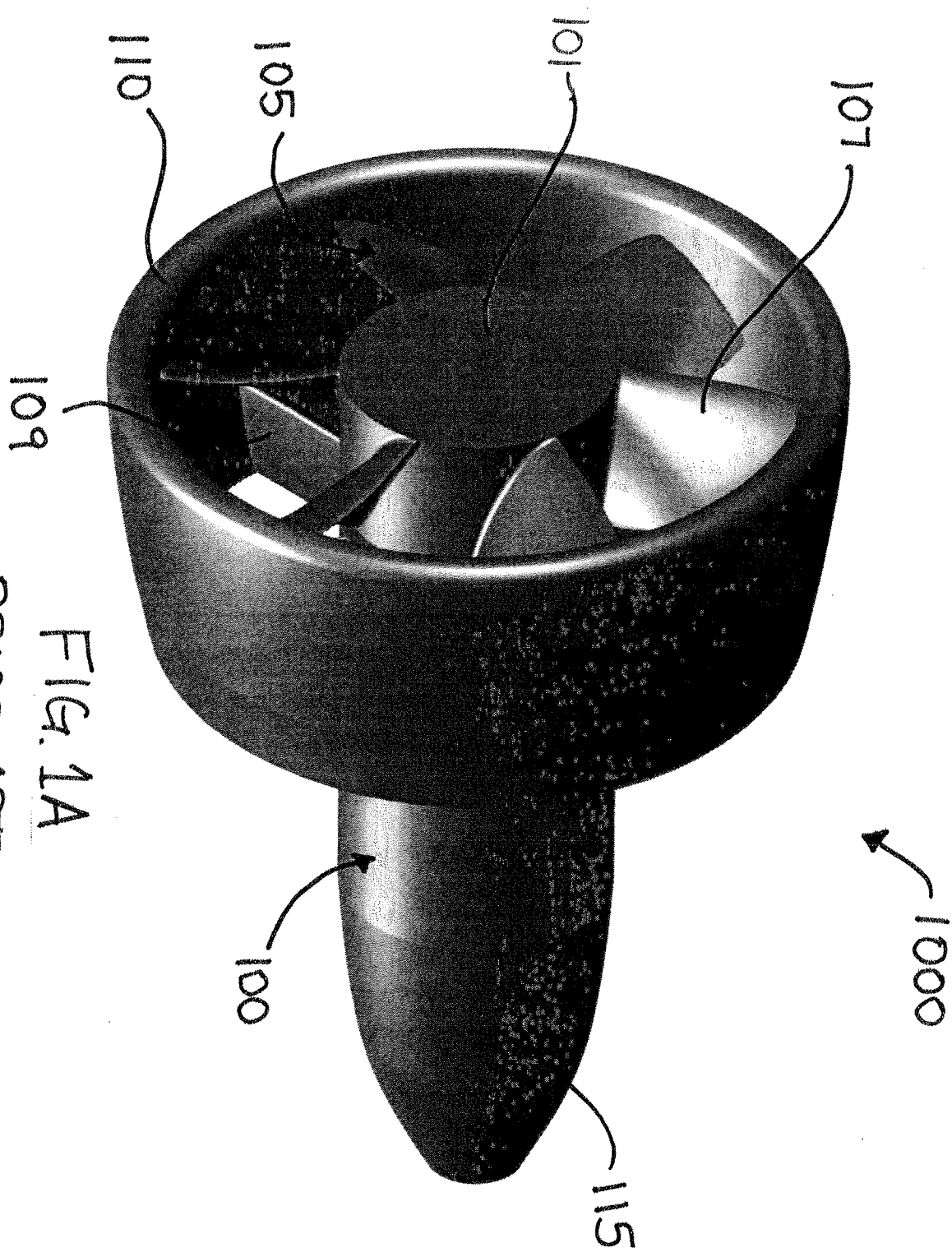
8. The ducted air rotor of claim 1, wherein the channel is a converging-diverging channel.

9. The ducted air rotor of claim 1, wherein the second duct is staionarily coupled to the first duct.
10. The ducted air rotor of claim 1, wherein the first duct and the second duct are concentrically oriented.
11. The ducted air rotor of claim 1, wherein the first duct and the second duct are eccentrically oriented.
12. The ducted air rotor of claim 11, wherein the second duct is axially movable with respect to the first duct to adjust a portion of the width of the channel.
13. The ducted air rotor of claim 1, wherein the second duct is longer than the first duct.
14. The ducted air rotor of claim 1, wherein the second duct is shorter than the first duct.

ABSTRACT

A double-ducted fan includes a hub, a rotor fan having a plurality of blades rotatably coupled to the hub, a first duct, a second duct, and a channel defined between the first duct and second duct. The first duct circumscribes the rotor fan and the second duct circumscribes at least a portion of the first duct. The second duct can be oriented axially upward such that there is an axial distance is between the leading edges of the first duct and second duct. The channel can be configured to direct air flow cross-wise to the first duct over a top of the first duct into the inlet side of the fan. The second duct can be movable relative to the first duct to adjust at least a portion of the channel. The length of the first duct can be different from the length of the second duct.

FIG. 1A
PRIOR ART



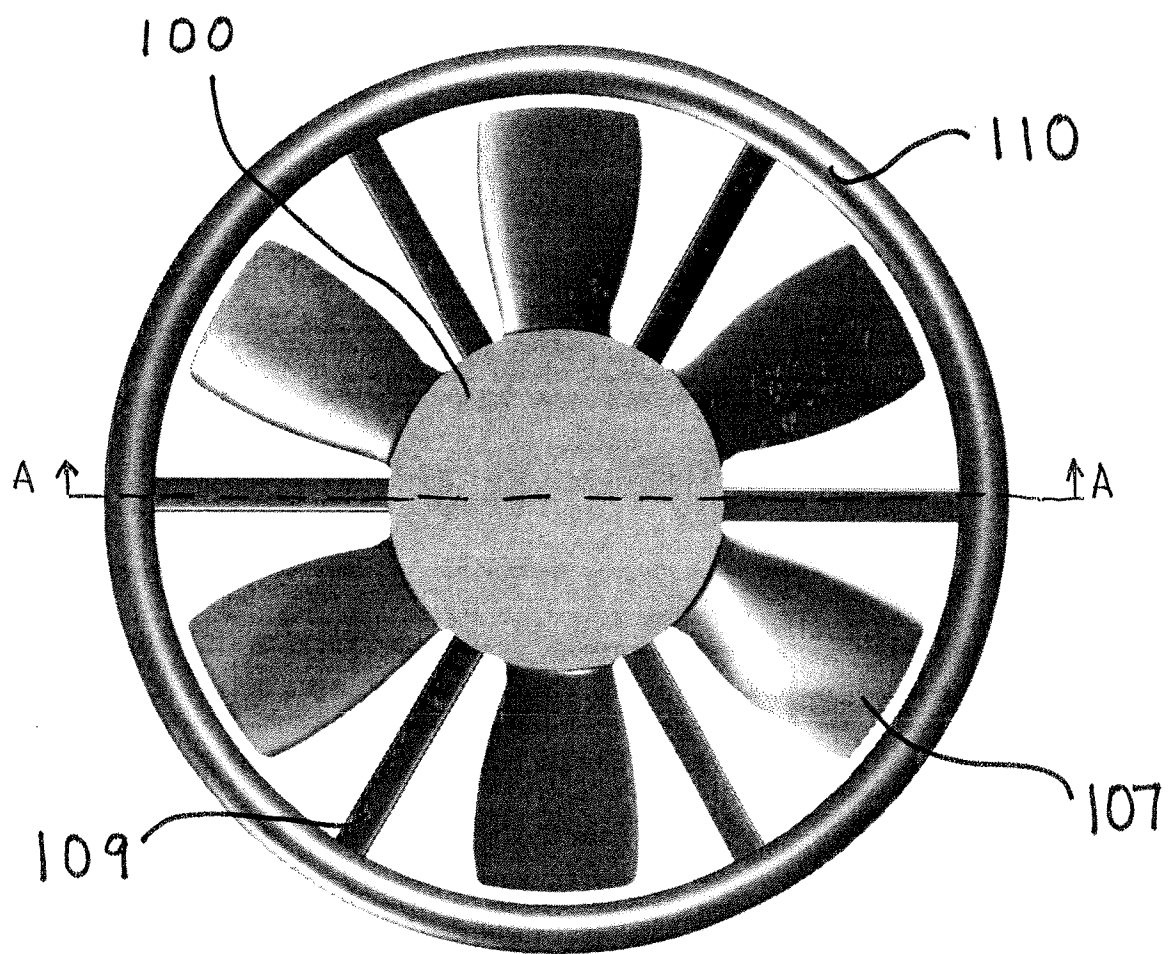


FIG. 1B
PRIOR ART

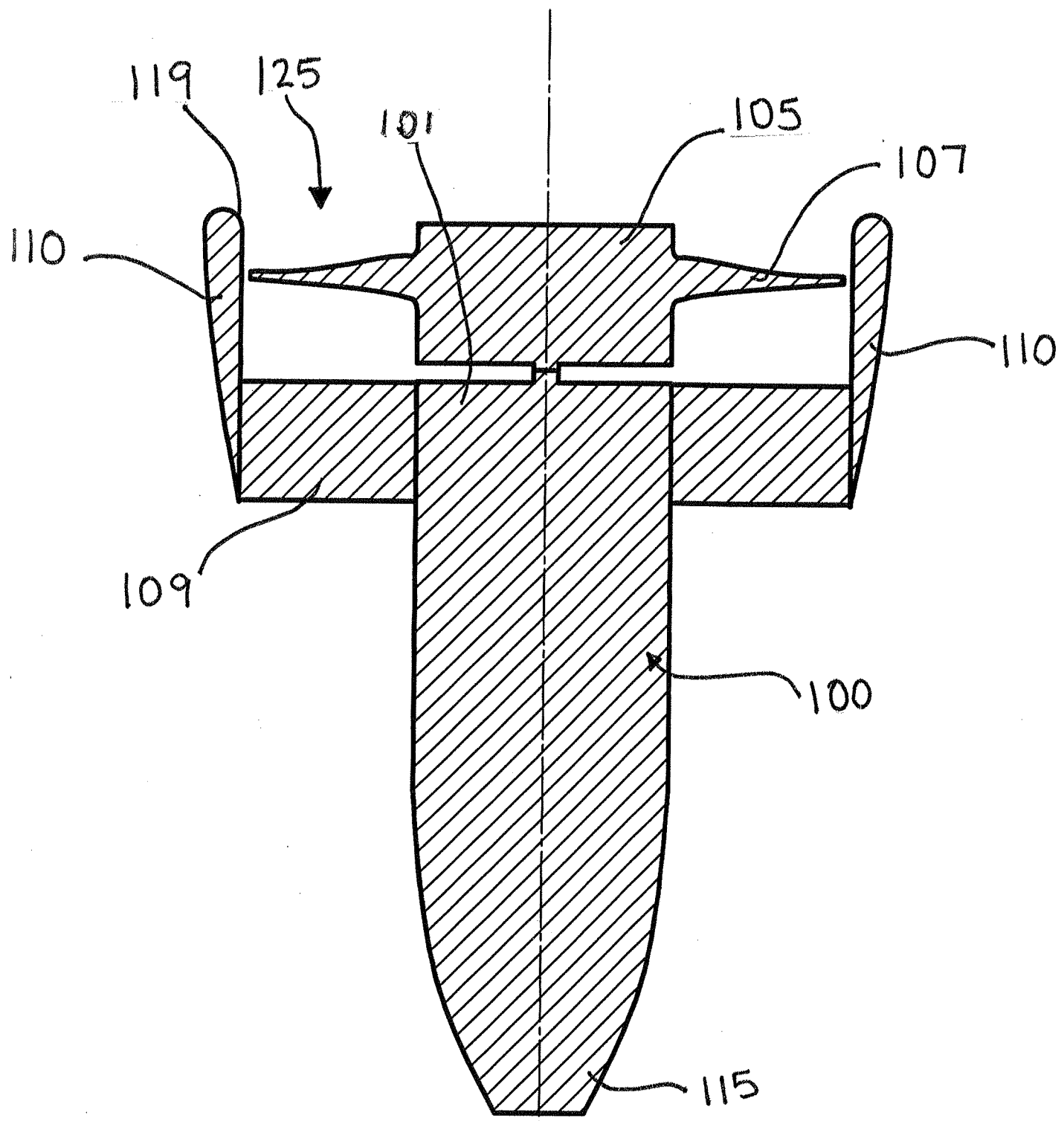


FIG. 1C
PRIOR ART

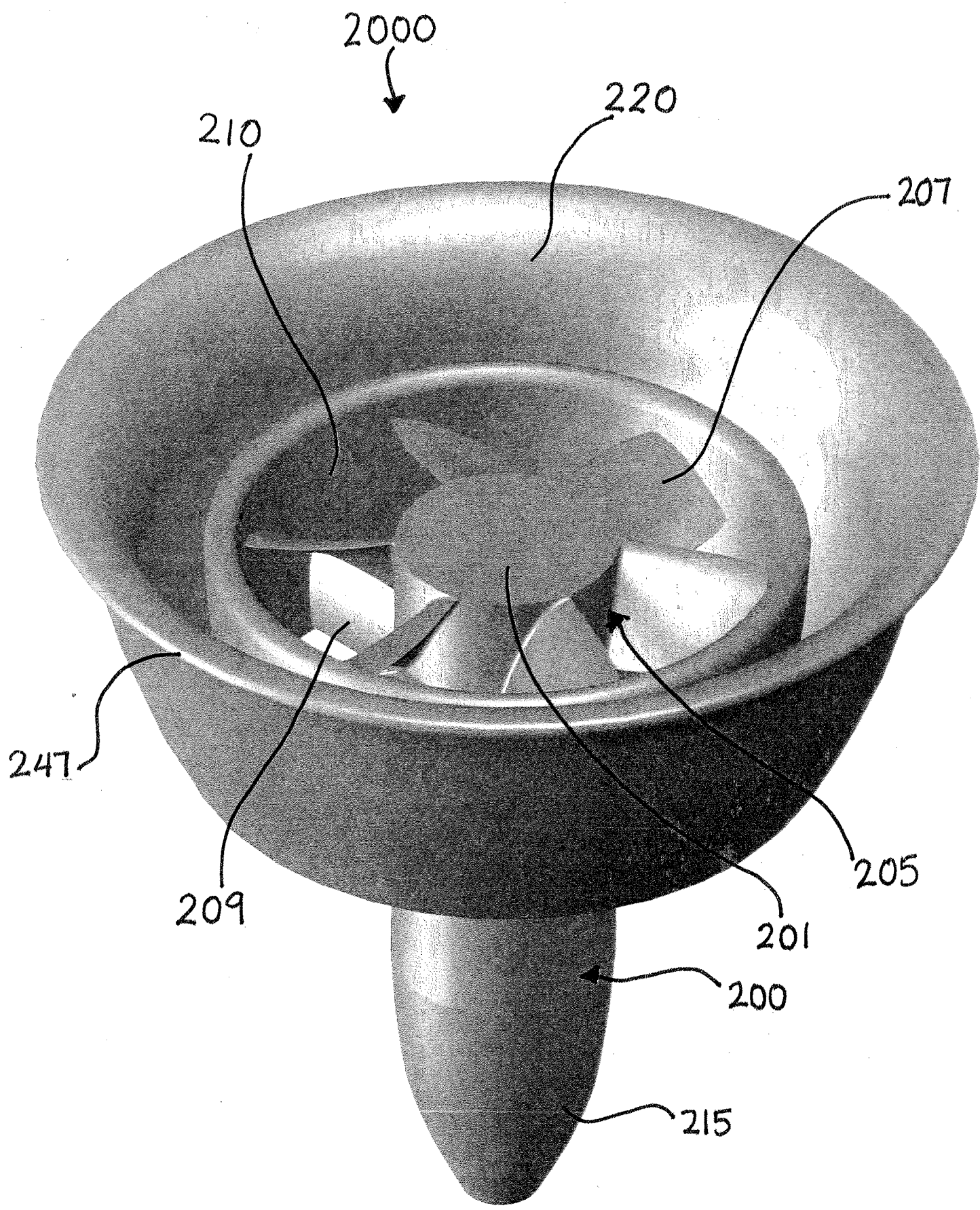


FIG. 2A

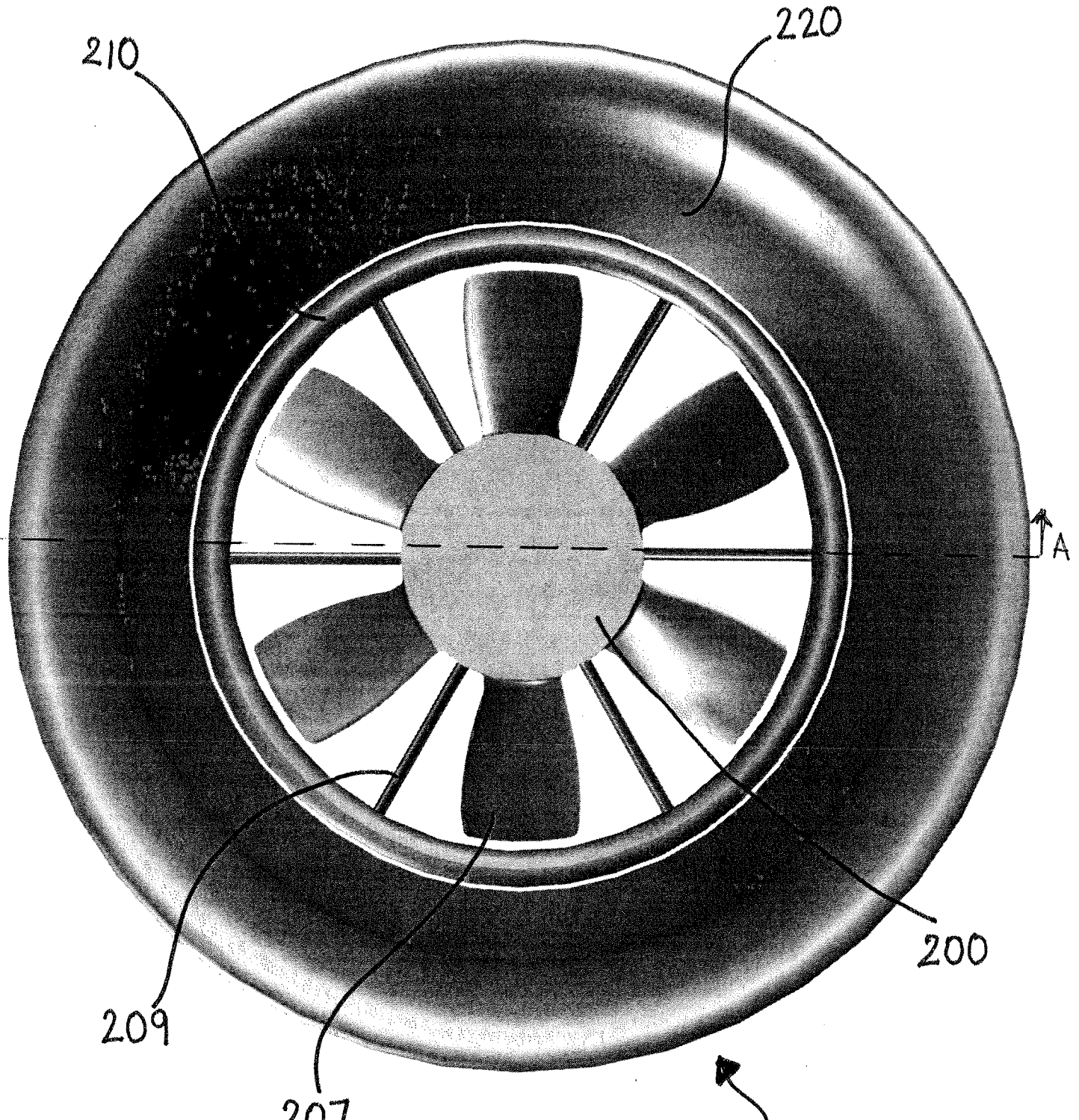


FIG. 2B

2000

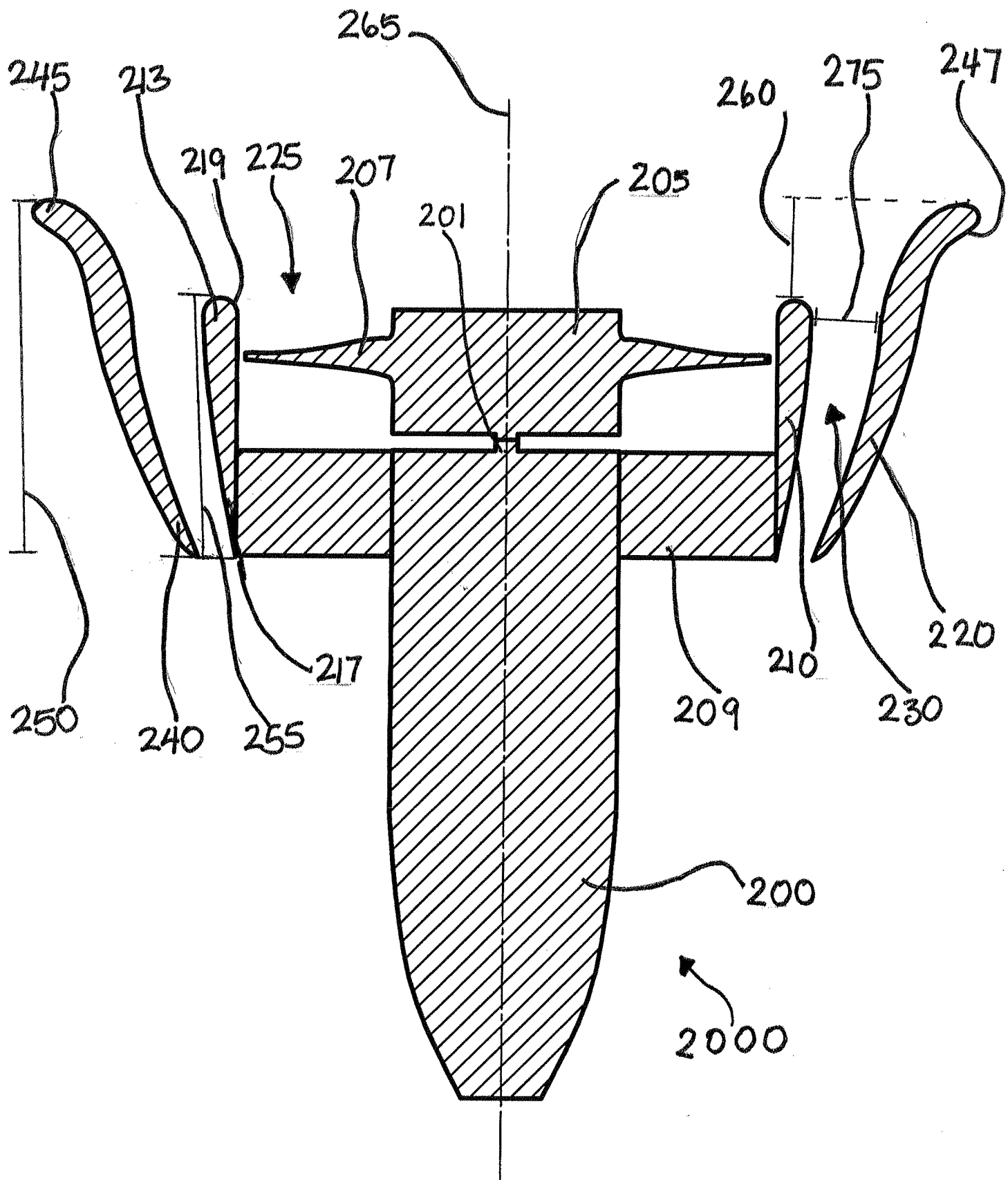


FIG. 2C

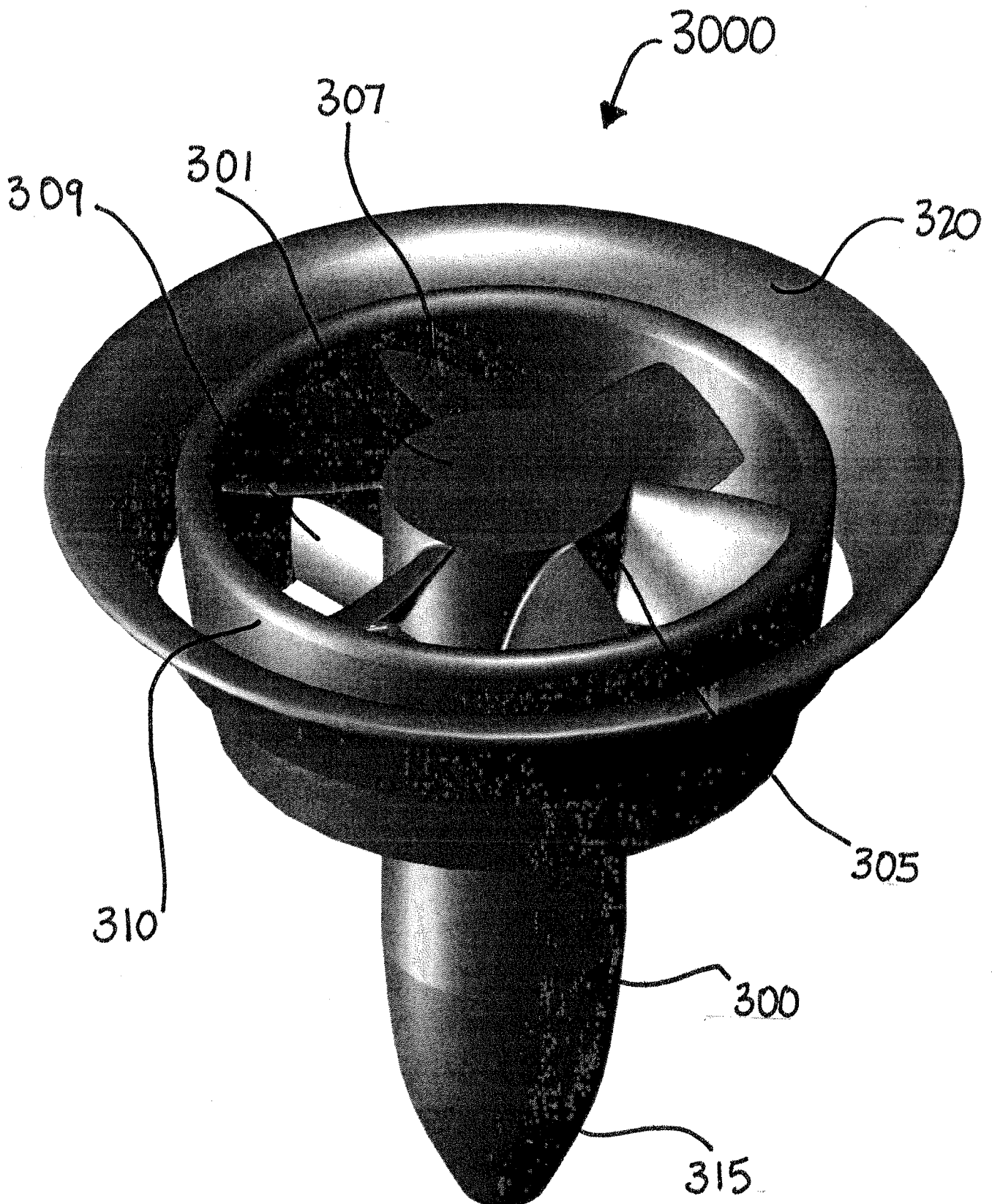


FIG. 3A

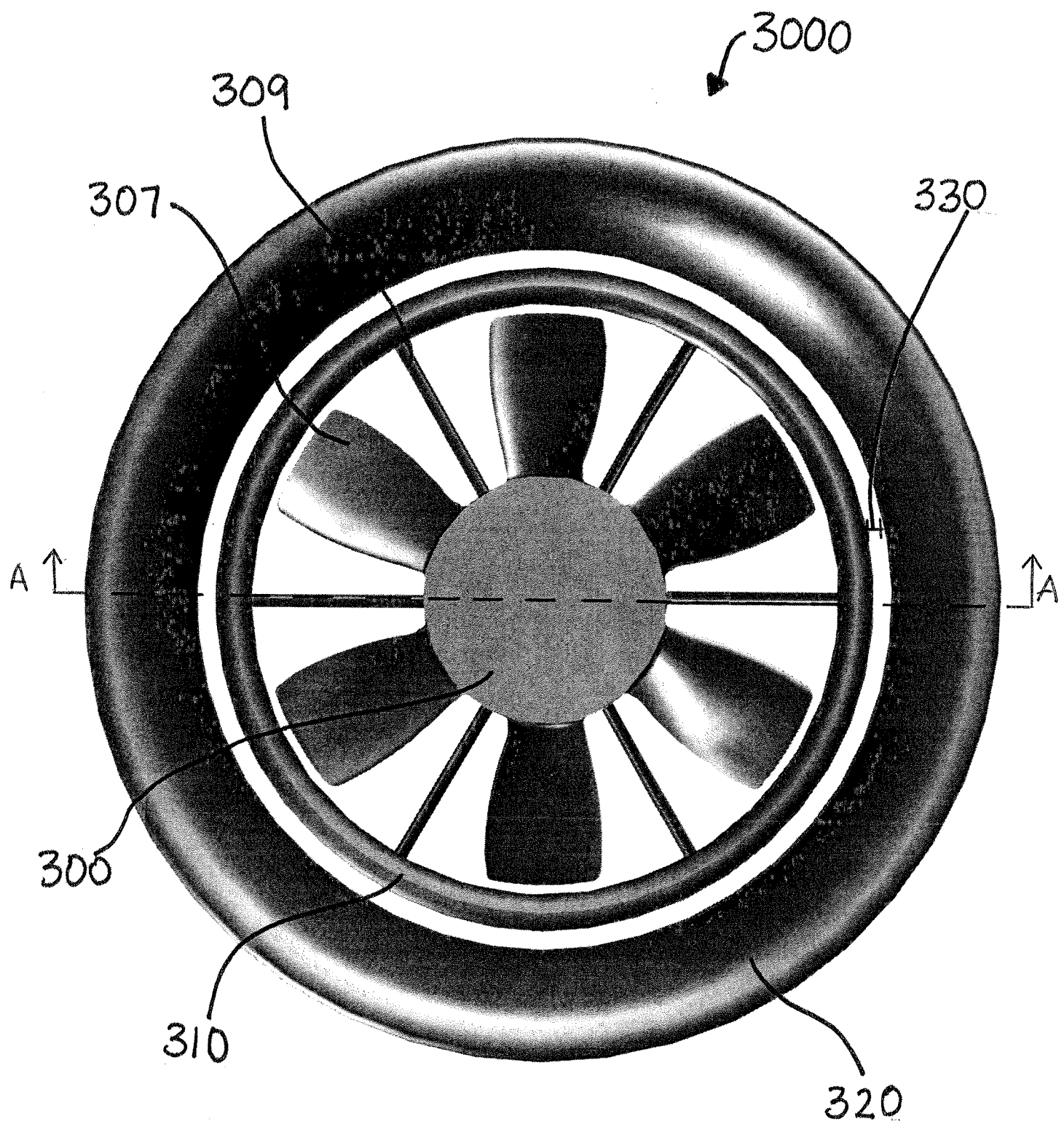


FIG. 3B

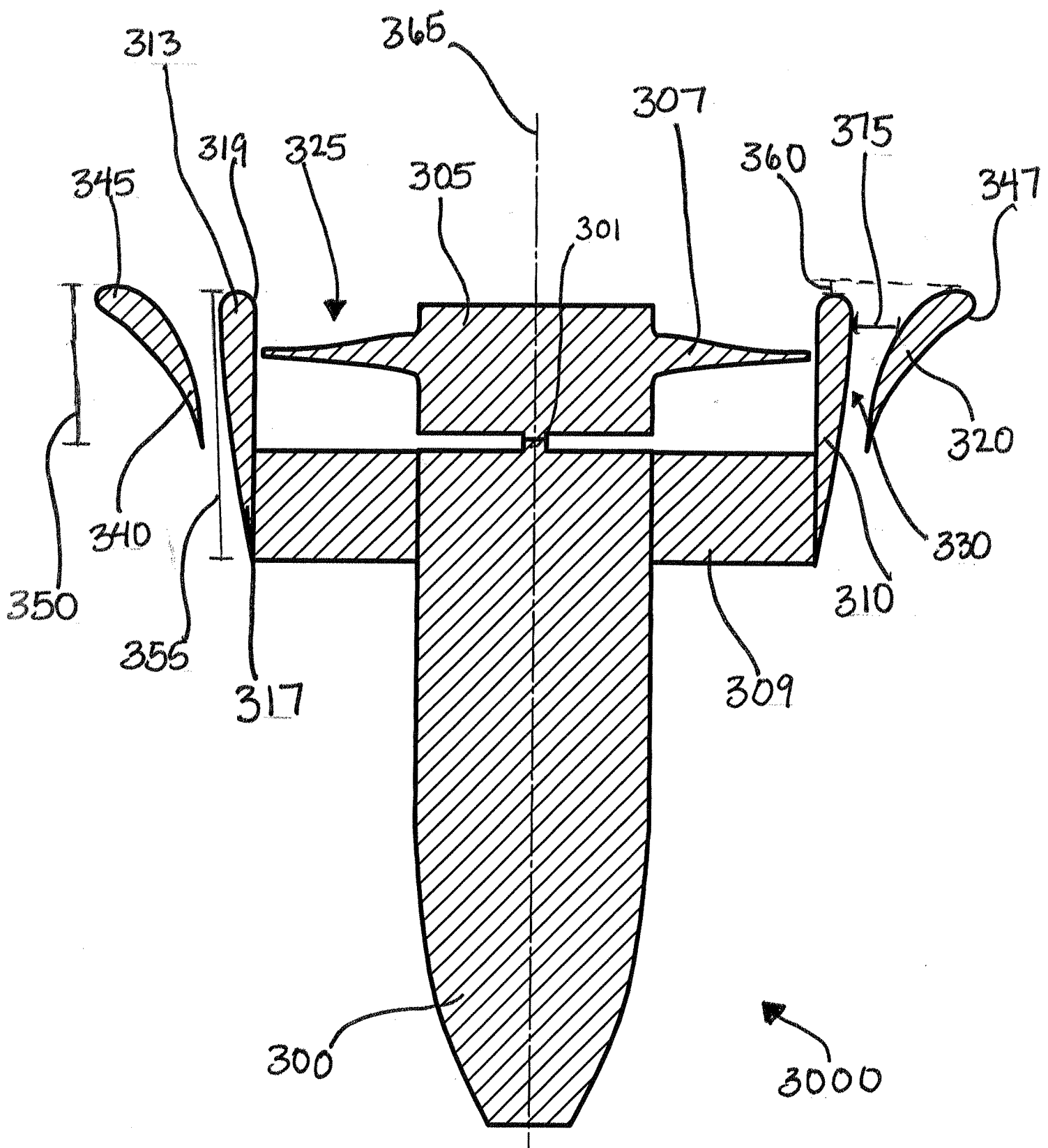


FIG. 3C

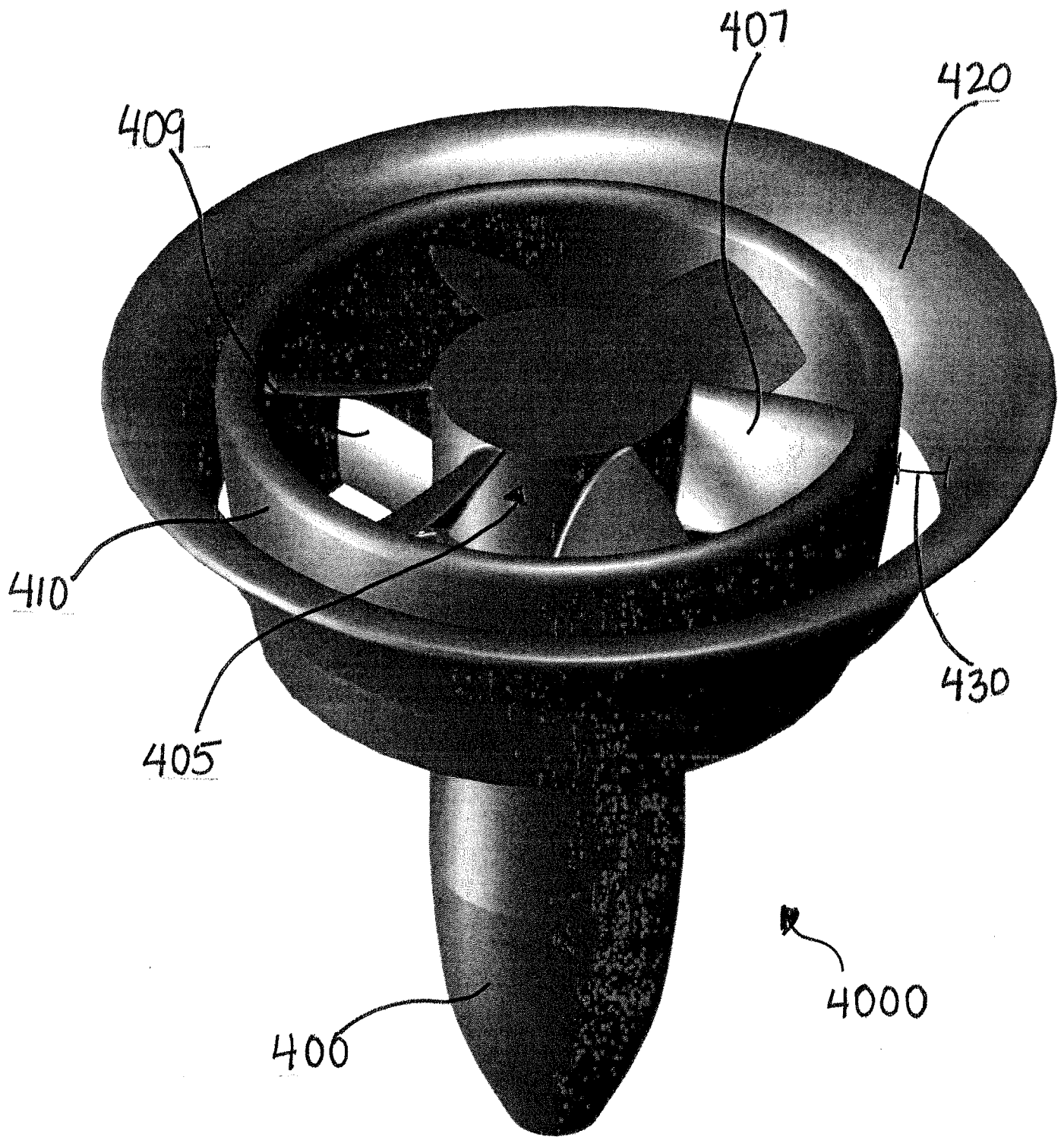


FIG. 4A

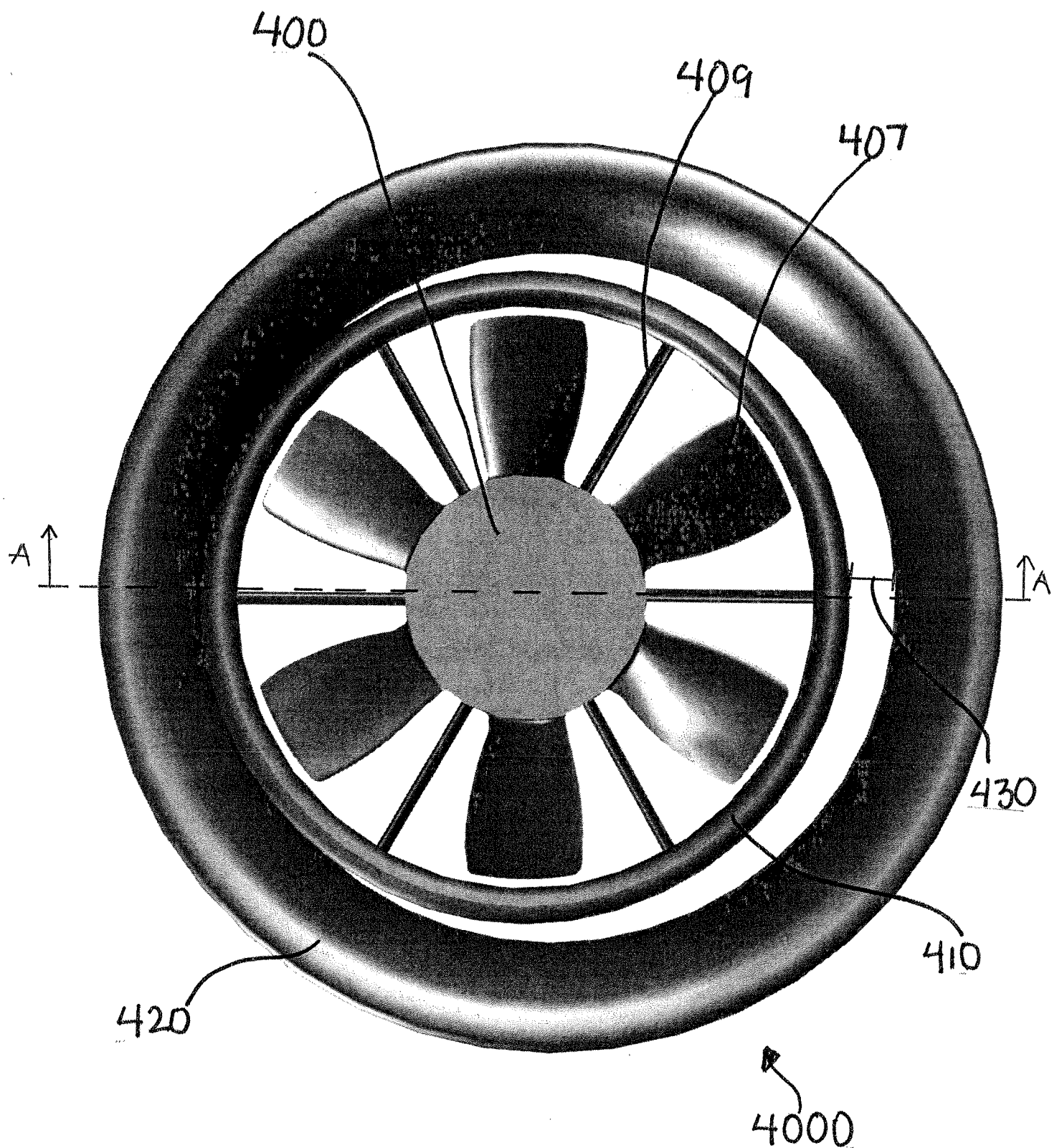


FIG. 4B

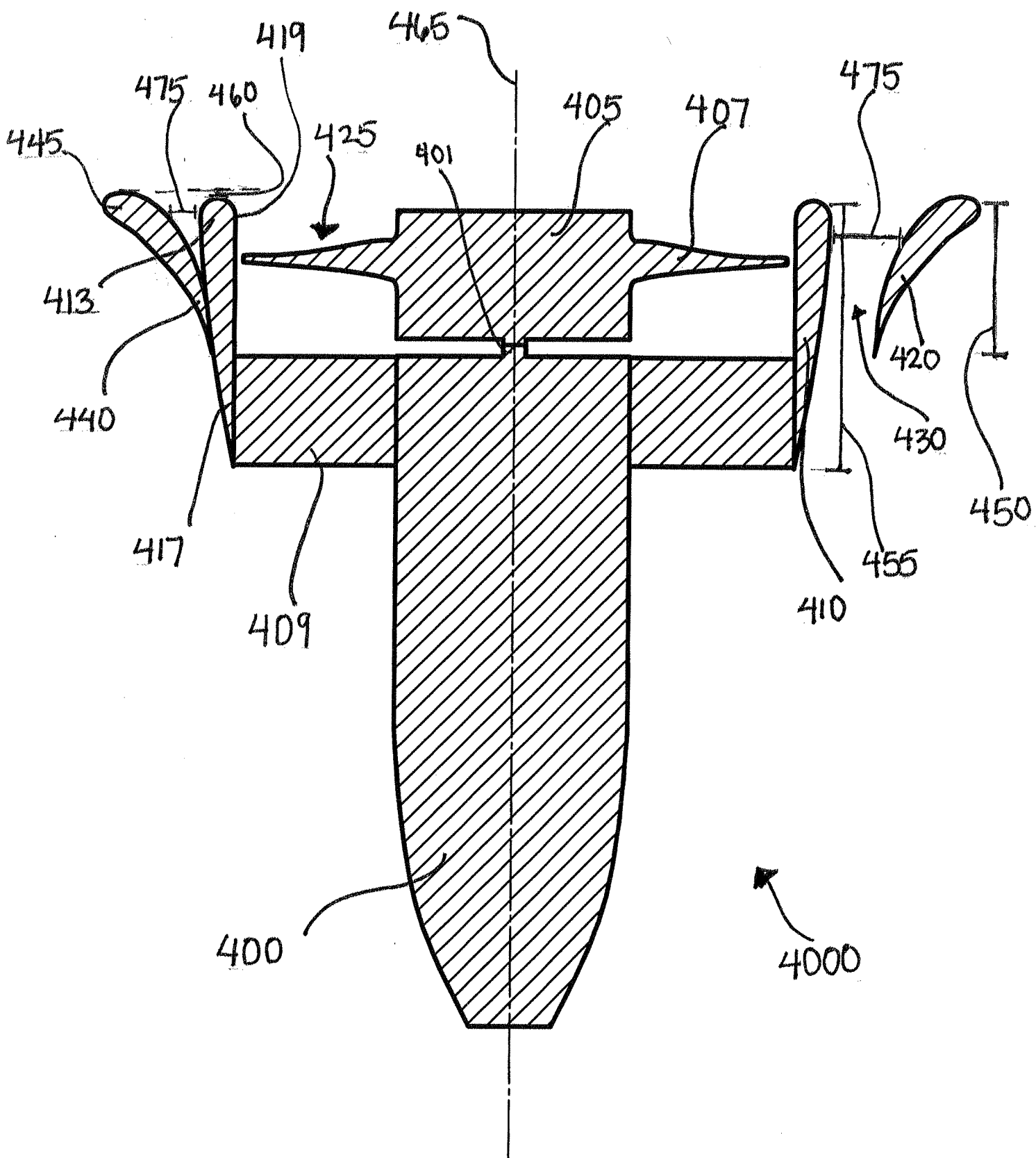


FIG. 4C

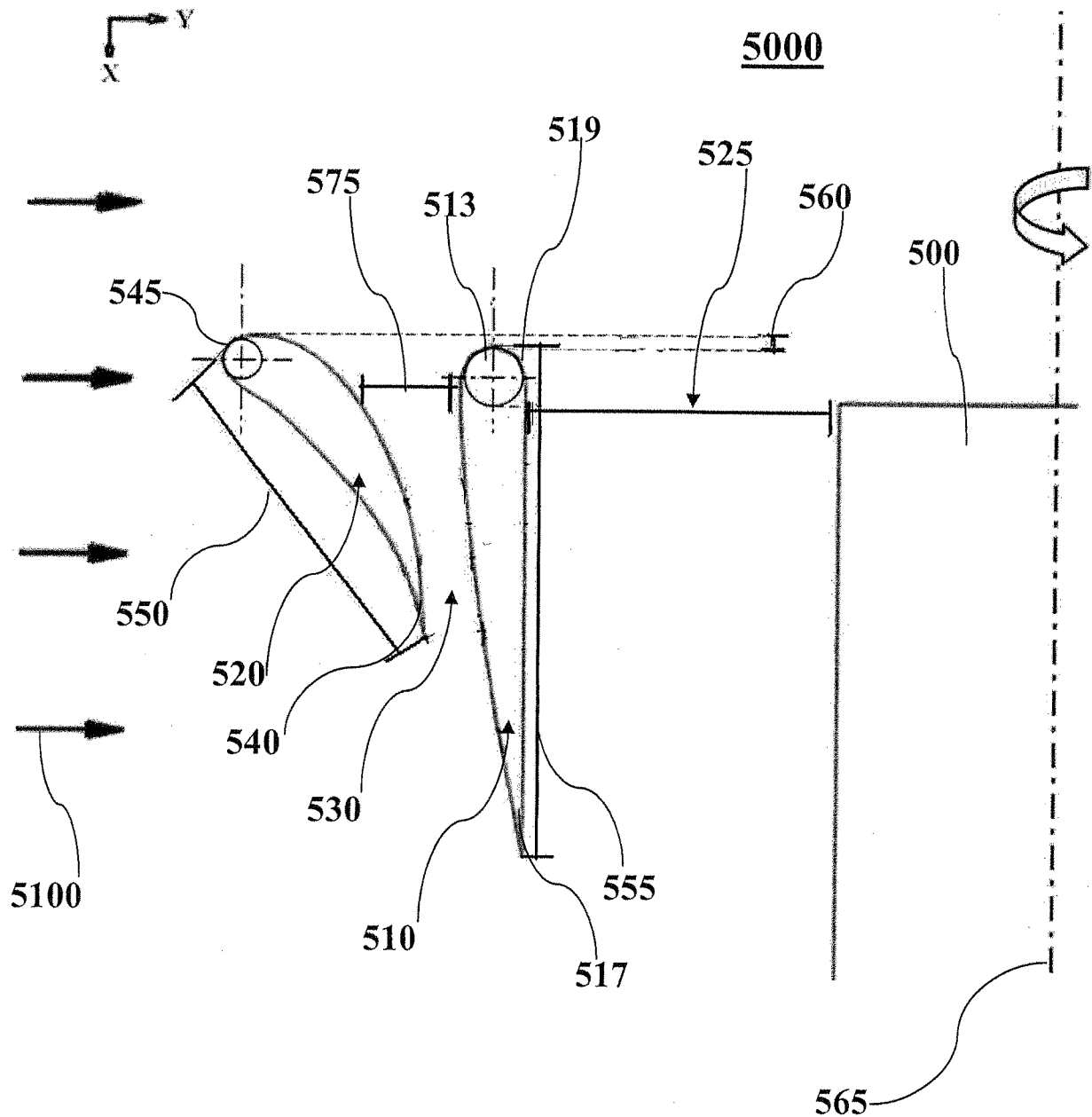


FIG. 5